



**MINISTRY OF EDUCATION**  
**POLITEHNICA University of Bucharest**  
**Doctoral School of Industrial Engineering and**  
**Robotics**

**Maria-Roxana N.I. MARINESCU**

**PhD THESIS SUMMARY**

**MANUFACTURING PROCESSES OF  
MICRO-ELECTRO-MECHANICAL-  
SYSTEMS WITH APPLICATIONS IN  
MEDICINE**

*PhD Supervision,*  
**Prof. Univ. Habil. Dr. Eng. Liviu-Daniel GHICULESCU**



**POLITEHNICA University of Bucharest**

**Maria-Roxana N.I. MARINESCU**

**PhD THESIS SUMMARY**

**MANUFACTURING PROCESSES OF  
MICRO-ELECTRO-MECHANICAL-  
SYSTEMS WITH APPLICATIONS IN  
MEDICINE**

**PhD Evaluation Board**

President	Prof.univ.dr.eng. Cristian-Vasile DOICIN	POLITEHNICA University of Bucharest
PhD supervisor	Prof.univ.dr.eng. Liviu-Daniel GHICULESCU	
Referent	Prof.univ.dr.eng. Nicolae IONESCU	POLITEHNICA University of Bucharest
Referent	Prof.univ.dr.eng. Oana DODUN- DES-PERRIERES	Technical University “Gheorghe Asachi” from Iași
Referent	CS1, dr.fiz. eng. Mărioara AVRAM	National Institute for Research and Development in Microtechnologies – IMT Bucharest

## CONTENT

	Thesis	Summary
<b>FOREWARD</b> .....	7	
<b>INTRODUCTION</b> .....	10	6
<b>PART ONE. ANALYSIS OF THE CURRENT STAGE REGARDING THE DEVELOPMENT OF MICRO-ELECTRO-MECHANICAL SYSTEMS</b> .....	13	8
<b>CHAPTER 1. THEORETICAL CONCEPTS REGARDING MICRO-ELECTRO-MECHANICAL SYSTEMS</b> .....	13	8
<b>1.1. Classification of Micro-Electro-Mechanical Systems components</b> .....	16	9
1.1.1. Microsensors .....	17	
1.1.2. Microactuators .....	17	
1.1.3. Integrated microsystems.....	17	
<b>1.2. Micro-Electro-Mechanical Systems with integrated biological functions</b> .....	18	9
<b>1.3. Effects of the environment on micro-electro-mechanical systems</b> .....	21	
<b>1.4. Conclusions</b> .....	21	
<b>CHAPTER 2. MATERIALS USED FOR THE MANUFACTURE OF MICRO-ELECTRO-MECHANICAL SYSTEM</b> .....	22	9
<b>2.1. Materials used as substrate</b> .....	23	9
<b>2.2. Materials used for deposition</b> .....	24	10
<b>2.3. Conclusions</b> .....	26	
<b>CHAPTER 3. TECHNOLOGIES FOR MANUFACTURING MICRO-ELECTRO-MECHANICAL SYSTEMS</b> .....	27	10
<b>3.1. Photolithography</b> .....	27	
3.1.1. General considerations .....	27	
3.1.2. Specific phenomena and performance factors of photolithography .....	28	
3.1.3. Specific applications regarding the photolithography technique .....	29	
3.1.4. Installations and equipment for the photolithography process .....	30	
<b>3.2. Chemical microprocessing technologies</b> .....	33	
3.2.1. General considerations .....	33	
3.2.2. Specific phenomena and performance factors of chemical corrosion processing .....	33	
3.2.3. Specific corrosion applications .....	34	
<b>3.3. Laser processing technologies</b> .....	35	
3.3.1. General considerations .....	35	
3.3.2. Specific phenomena of laser processing .....	36	
3.3.3. Specific laser applications .....	37	
3.3.4. Laser installations and equipment .....	38	
<b>3.4. Electron beam processing technologies</b> .....	40	
3.4.1. General considerations .....	40	
3.4.2. Specific phenomena .....	40	
3.4.3. Specific applications .....	41	
3.4.4. Electron beam processing plants and equipment.....	42	
<b>3.5. Ion beam processing technologies</b> .....	42	
3.5.1. General considerations .....	42	
3.5.2. Physico-chemical phenomena in ion beam processing.....	43	
3.5.3. Applications of ion beam processing.....	44	
3.5.4. Equipment and installations.....	44	
<b>3.6. Plasma processing technologies</b> .....	45	
3.6.1. General considerations .....	45	
3.6.2. Specific phenomena .....	45	
3.6.3. Specific applications .....	46	

---

3.6.4. Equipment and installations.....	47
<b>CHAPTER 4. MICROFLUIDICS AND “LAB-ON-A-CHIP” DEVICES .....</b>	<b>49 11</b>
<b>4.1. Microfluidics used to separate cells .....</b>	<b>49 11</b>
4.1.1. Classification and number of blood cells.....	49 11
4.1.2. The importance of lymphocytes in the blood .....	53 11
<b>4.2. Microfluidic devices construction .....</b>	<b>54 12</b>
<b>4.3. Types of microfluidic circuits .....</b>	<b>56 12</b>
<b>4.4. Studiul actual al dispozitivelor “Lab-On-a-Chip” .....</b>	<b>57</b>
4.4.1. "Lab-On-a-Chip" devices for the determination of T lymphocytes .....	60
4.4.2. "Lab-On-a-Chip" devices for the determination of circulating tumor cells.....	63
<b>4.5. Conclusions.....</b>	<b>65</b>
<b>PART TWO. CONTRIBUTIONS REGARDING THE DEVELOPMENT OF MICRO-ELECTRO-MECHANICAL SYSTEMS WITH APPLICATIONS IN MEDICINE .....</b>	<b>66 12</b>
<b>CHAPTER 5. OBJECTIVES, RESEARCH DIRECTIONS AND METHODOLOGY ADDRESSED IN THE DOCTORAL THESIS.....</b>	<b>66 12</b>
<b>5.1. Synthesis of critical aspects regarding the current state of micro-electro-mechanical systems with applications in medicine .....</b>	<b>66 12</b>
<b>5.2. Objectives of the doctoral thesis .....</b>	<b>67 14</b>
<b>5.3. Research directions and research methodology of the doctoral thesis .....</b>	<b>69 15</b>
<b>CHAPTER 6. RESEARCH ON THE DESIGN, MODELING AND SIMULATION OF A MICRO-ELECTRO- MECHANICAL DEVICE FOR DETERMINING T LYMPHOCYTES, EXPERIMENTAL MODEL.....</b>	<b>70 16</b>
<b>6.1. General data .....</b>	<b>70 16</b>
<b>6.2. Establishing the functions and the functional structure of the product .....</b>	<b>70 16</b>
<b>6.3. Technological data obtained in the laboratory .....</b>	<b>74 17</b>
<b>6.4. Establishing the shape of microfluidic pathways .....</b>	<b>74 17</b>
<b>6.5. Design of the micro-electro-mechanical device, experimental model.....</b>	<b>76 18</b>
<b>6.6. Modeling the manufacturing process of the micro-electro-mechanical device, experimental model.....</b>	<b>92 20</b>
<b>6.7. Computer modeling and simulation of microfluidic flow in the micro-electro-mechanical device, experimental model.. ..</b>	<b>100 20</b>
<b>6.8. Conclusions.....</b>	<b>104</b>
<b>CHAPTER 7. MANUFACTURE OF A MICRO-ELECTRO-MECHANICAL DEVICE, EXPERIMENTAL MODEL.....</b>	<b>105 22</b>
<b>7.1. Writing the masks .....</b>	<b>105</b>
<b>7.2. The actual manufacture of the device, experimental model.....</b>	<b>108 22</b>
7.2.1. Silicon wafer used as substrate .....	108 22
7.2.2. Silicon oxide deposition.....	109 22
7.2.3. Photolithography for the first mask .....	111 23
7.2.4. Deposition of the titanium-gold layer .....	117 24
7.2.5. Lift-off removal of the photoresist for the first mask .....	119 24
7.2.6. Photolithography process for the second mask.....	120 25
7.2.7. Deposition of the silver layer .....	121 25
7.2.8. Removal of the photoresist by lift-off for the second mask.....	121 25
7.2.9. Photolithography process for the third mask .....	129 26
7.2.10. Polydimethylsiloxane cover deposition.....	134 28
<b>7.3. Conclusions .....</b>	<b>138</b>
<b>CHAPTER 8. DEVICE TESTING, EXPERIMENTAL MODEL.....</b>	<b>140 29</b>
<b>8.1. Testing methodology.....</b>	<b>140 29</b>
<b>8.2. Verificarea trecerii curentului electric .....</b>	<b>142</b>
<b>8.3. Electrochemical impedance spectroscopy.....</b>	<b>143 30</b>

---

<b>8.4. Conclusions</b> .....	149
<b>CHAPTER 9. MANUFACTURE AND TESTING OF THE IMPROVED PROTOTYPE OF THE MICRO-ELECTRO-MECHANICAL DEVICE</b> .....	151 33
<b>9.1. Problems appeared in the manufacture of the micro-electro-mechanical device, experimental model</b> .....	151 33
<b>9.2. Improvements in the manufacturing process of the micro-electro-mechanical device</b> .....	152 33
9.2.1. Silver deposition improvements .....	152 34
9.2.2. Improvements needed to increase the adhesion of the SU-8 photoresist .....	152 34
<b>9.3. Execution of the improved prototype of the micro-electro-mechanical device</b> .....	152 34
9.3.1. Design of the micro-electro-mechanical device, improved prototype .....	154 35
9.3.2. Modeling of the manufacturing process of the micro-electro-mechanical device, improved prototype .....	160 37
9.3.3. The manufacturing process of the masks .....	165 37
9.3.4. Execution of the micro-electro-mechanical device, improved prototype .....	167 38
<b>9.4. Testing the improved prototype of the micro-electro-mechanical device</b> .....	175 41
9.4.1. Sensor stability .....	176 42
9.4.2. Microfluidic flow testing.....	177 43
9.4.3. Testing the sensor's functionality with electrochemical impedance spectroscopy.....	178 43
<b>9.5. Integration of the microfluidic chip into a portable device</b> .....	180 44
<b>9.6. Mechanical-climatic reliability tests for the micro-electro-mechanical device</b> .....	181 45
<b>9.7. Development of a humidity sensor for monitoring the storage conditions of the micro-electro-mechanical device</b> .....	188 48
<b>9.8. Conclusions</b> .....	197
<b>CHAPTER 10. FINAL CONCLUSIONS, PERSONAL CONTRIBUTIONS AND FUTURE RESEARCH DIRECTIONS</b> .....	200 48
<b>10.1. Final conclusions</b> .....	200 48
<b>10.2. Original contributions</b> .....	202 50
<b>10.3. Future directions of research</b> .....	205 54
<b>10.4. Valorification of the research results</b> .....	206 54
<b>SELECTIVE BIBLIOGRAPHY</b> .....	207 55
<b>APPENDIX 1. LIST OF ABBREVIATIONS</b> .....	220 58
<b>APPENDIX 2. SPECIFIC TERMS</b> .....	224
<b>APPENDIX 3. LIST OF FIGURES</b> .....	225
<b>APPENDIX 4. LIST OF TABLES</b> .....	233
<b>APPENDIX 5. PAPERS PUBLISHED IN VOLUMES OF SOME ISI-INDEXED CONFERENCES</b> .....	234
<b>APPENDIX 6. PAPERS PUBLISHED IN ISI INDEXED JOURNALS</b> .....	235
<b>APPENDIX 7. PAPERS PUBLISHED IN VOLUMES OF SOME CONFERENCES INDEXED IN INTERNATIONAL DATABASES</b> .....	236
<b>APPENDIX 8. Papers PUBLISHED IN JOURNALS INDEXED IN INTERNATIONAL DATABASES</b> .....	237
<b>APPENDIX 9. BOOKS / BOOK CHAPTERS</b> .....	239
<b>APPENDIX 10. CONFERENCE ATTENDANCE - POSTERS, BOOK OF ABSTRACTS</b> .....	240
<b>APPENDIX 11. PATENT APPLICATIONS</b> .....	242
<b>APPENDIX 12. AWARDS</b> .....	243

## INTRODUCTION

Technology represents the processes, methods and operations used in order to obtain a particular product. Microelectronics and nanoelectronics are two areas with a significant contribution to the technological progress. The research-development-innovation activities carried out within the two fields, have produced valuable results of reference for the current doctoral thesis: micro-electro-mechanical systems (MEMS).

MEMS are miniaturized systems with small dimensions and weights that can be easily integrated into various commercial applications. These small aids with high technology are more and more present in our daily lives. Smart structures allow us to control better the environment and help us increase the energy efficiency of devices. All the applications that belong to the current era, Industry 4.0 (the fourth industrial revolution), integrate the following types of elements: sensor, microprocessor, database and actuator.

Within the doctoral thesis “**Manufacturing processes of micro-electro-mechanical systems with applications in medicine**” in the field of Industrial Engineering, a “lab-on-a-chip” type device to where T lymphocytes in the blood can be determined was designed, modeled, simulated and manufactured. Therefore, the doctoral thesis can be included in the field of bioengineering. In this branch of science, concepts are developed from the molecular level to the systemic level, with the role of developing new biological products, materials, medical devices for diagnosis, prevention and treatment of diseases, as it is the case of the device resulting from this doctoral thesis. The field of medical engineering is closely related to the following subfields: biomechanics, biomaterials, electronics, mechatronics, biophysics, medical imaging, telemedicine, nanotechnology, cellular engineering and genetics, therefore, it is a field with obvious multidisciplinary character.

The doctoral thesis is organized in two main parts: (1) the current state and (2) contributions on the development of micro-electro-mechanical systems with applications in medicine and is structured in 10 chapters, comprising 219 pages, 286 figures, 28 tables, 248 bibliographical references and 12 annexes, in total, 244 pages.

The micro-electro-mechanical devices in the thesis were made within the National Institute for Research and Development in Microtechnologies – IMT Bucharest.

The first chapter: “**Theoretical concepts regarding micro-electro-mechanical systems**” presents the evolution of researches in the field of micro-electro-mechanical devices and, implicitly, some fields of research and applications in the production of MEMS devices.

In the second chapter of the thesis: “**Materials used for the manufacture of micro-electro-mechanical systems**”, both materials were used as a substrate; those used for deposition in the construction of MEMS are described and analyzed.

A particular attention is given to chapter three, which consists in “**Technologies for the manufacture of micro-electro-mechanical systems**”. In this chapter, specific technologies for the manufacture of micro and nanostructures are described: processing by photolithographic techniques, laser processing, plasma processing, chemical processing, ion and electron beam processing. For each type of processing, specific phenomena, performance factors, specific applications are described and models of modern equipment and work installations are presented.

The fourth chapter of the thesis: “**Microfluidics and Lab-On-a-Chip devices**” is intended to be a synthesis of the analysis performed on the latest papers published in the field. Microfluidic devices are presented for two detectable cell types: circulating tumor cells (CTCs) and T lymphocytes. A literature review was performed on Lab-On-a-Chip microfluidic devices. Thus, the main requirements imposed on both materials and obtaining technologies were identified, in order to achieve a device for detecting T lymphocytes in the blood. The advantages of using cellular detection devices are highlighted.

Chapter five: “**Objectives, research directions and methodology addressed in the doctoral thesis**” presents, in the first part, the synthesis of critical aspects resulting from the study of MEMS devices in the current state. On this basis, the objectives of the thesis, the directions and the research methodology were established, which led to the achievement of these objectives.

Chapter six of the thesis: “**Research on the design, modeling and simulation of a micro-electro-mechanical device for the determination of T lymphocytes, experimental model**” presents the design, modeling and simulation elements of the device. Before carrying out these research and development stages, it is necessary to know certain essential elements about cells. These data were obtained by experimental chemical studies from INCD for Microtechnology - IMT.

The design of the device was made with the help of the CleWin5 program, after the dimensions and framing of the components on the microfluidic platform were established in advance. The modeling elements were obtained by using SEMulator 3D program, with which, the correctness of the design for the device was demonstrated and the parameters established in the design phase for the realization of the T lymphocyte detection device were validated. Simulation with the finite element method was realized in the dedicated program, Comsol Multiphysics. This was done for the microfluidic flows of the device. The results led to the proper manufacture of the micro-electro-mechanical device, validating the obtained model.

Chapter seven: “**Manufacture of a micro-electro-mechanical device, experimental model**” is the most significant chapter of the thesis. In this chapter all the manufacturing stages of the micro-electro-mechanical device are characterized in detail. The materials used are described, with details on their selection, the equipment that was used at each stage, the results of the intermediate inspections that took place at each stage and the final conclusions on the obtained device.

Chapter eight: “**Device testing, experimental model**” presents the tests performed both on the electrical response and on the response given by antigens and antibodies. These tests demonstrated the functionality of the device.

Chapter nine: “**Manufacture and testing of the improved prototype of the micro-electro-mechanical device**” is a comprehensive chapter, which presents the improved prototype of the micro-electro-mechanical device, after analysing the problems identified in the manufacturing process of the experimental model and establishing the new work stages.

For the improved prototype of the micro-electro-mechanical device, the design-modeling stages, the manufacturing stages, with the materials and equipment used and the testing stages are presented. Tests of fluid flow and verification of sensor functionality were performed, as in the previous phase of the experimental model. Moreover, the idea of device portability was presented, which gives it a huge advantage in the medical device market. To verify its resistance to the environment, vibration and thermal shock tests were performed, which are required for all portable devices.

Regarding the storage conditions of medical devices, the humidity factor was analyzed and the use of a new humidity sensor was proposed. Mechanical-thermal tests were also performed for this sensor. The response given by the sensor was one that allows the control of the storage conditions of the micro-electro-mechanical device made.

Chapter ten, “**Final Conclusions, Original Contributions and Future Research Directions**” is dedicated to the conclusions resulting from the completion of the doctoral thesis, as well as the original theoretical and applied contributions. The future research directions and the capitalization of the research and development results of the product and manufacturing process are also presented.

*Keywords: micro-electro-mechanical systems, microfluidic bio-devices, lab-on-a-chip, manufacturing, unconventional technologies.*

## PART ONE. ANALYSIS OF THE CURRENT STAGE REGARDING THE DEVELOPMENT OF MICRO-ELECTRO-MECHANICAL SYSTEMS

### CHAPTER 1. THEORETICAL CONCEPTS REGARDING MICRO-ELECTRO- MECHANICAL SYSTEMS

Micro-electro-mechanical systems (MEMS) are small integrated devices or systems that combine mechanical and electrical components created using microtechnological processes. These microsystems are chip-sized devices (sizes can range from a few micrometers to a few millimeters) that have the ability to detect data, process it and then transmit the information. They can act on a micro or even nano scale and can generate macro scale effects [M4], [P10]. MEMS are part of the Nanotechnology branch, they are made using nano and micro elements.

Micro and nanostructures have a wide range of applications in various fields (electrical, mechanical, biological, optical etc.). These small devices, which use state-of-the-art technologies, are found in almost everything around us. The first sector occupied by MEMS devices is the electronic industry, followed by the second major market: the auto sector [M20].

MEMS devices with integrated biological functions used for medical applications are called **bioMEMS**. In the surgical field, MEMS technology has the potential to not only improve the functionality of existing devices, but also to add new capabilities, which allows doctors to develop new techniques and perform completely new procedures [R2]. An astonishing demand for autonomous micro-devices in the medical field increases the need for miniaturized energy sources. BioMEMS applications include biomedical transducers, microfluidic devices, medical implants, microsurgical instruments and tissue engineering.

With the help of modern technology, man uses these microsystems in order to simplify his own life. Some of the examples used for this purpose are shown in Figs. 1.2 [B14], [Z2].

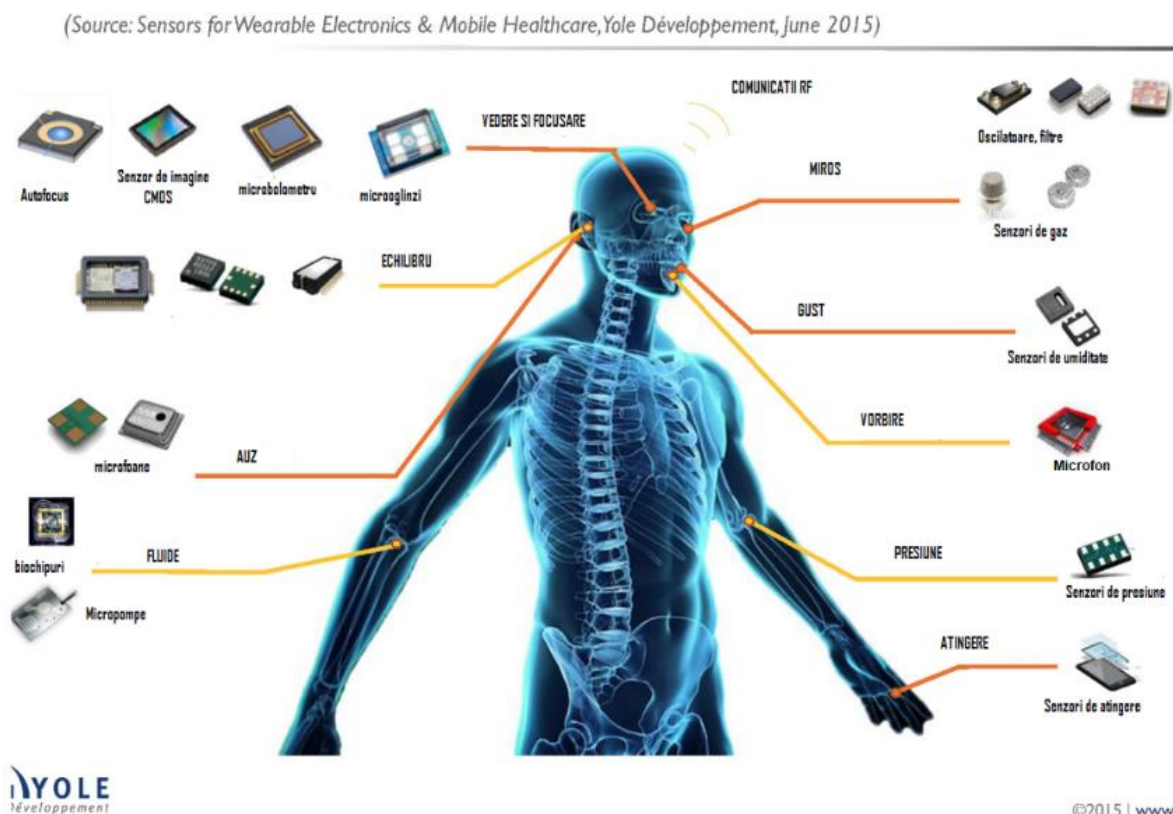


Fig. 1.2. MEMS devices used by humans [B14]

## 1.1. Classification of Micro-Electro-Mechanical Systems components

In general, MEMS are made of mechanical microstructures, microsensors, microactuators and microelectronic components, using materials with special properties (ferrous, piezo- etc.) [P10], [M32], [Z7], [M37].

## 1.2. Micro-Electro-Mechanical Systems with integrated biological functions

In designing and developing a suitable microdevice that can be used successfully in the medical field, it is necessary to have a balance between technological factors (measuring sensors and associated electronics) and human factors. Technological factors are represented by sensors that collect information about physiological parameters [B15]. If all these factors are taken into account, devices that ensure safety, efficacy and ease of use can be developed. These devices that interact with the human body can be divided into two categories: attachable devices and implantable devices [M24].

## CHAPTER 2. MATERIALS USED FOR THE MANUFACTURE OF MICRO-ELECTRO-MECHANICAL SYSTEMS

Designing a MEMS device that achieves a certain level of performance requires choosing the right materials. The selection of materials used in the functional manufacture of MEMS takes place according to their properties: piezoelectricity, electro- and magnetostriction, ferro- and para-electricity, ferroelasticity, magnetoresistance or pyroelectricity. For the microfabrication of MEMS devices used in medical services, the biocompatibility and incompatibility of the antimicrobial activity of the materials are evaluated [S12]. From all the studies performed, it was found that two of the properties that are of great interest in the manufacture of MEMS are the mechanical-elastic properties. The other properties, such as thermal, electrical, chemical or optical properties, depend more on the specific applications for which the MEMS device is used [S12], [M24], [S14].

The materials used in the manufacture of MEMS fall into two categories:

- (a) materials used as substrate;
- (b) materials used for deposition.

### 2.1. Materials used as substrate

A MEMS device is made of two or more materials and very rare of a single material. The most important material used as a substrate in MEMS manufacture is silicon (Si) [P10].

The other materials beside silicon (Fig. 2.3.) that can be used to make MEMS are: quartz; glass; polymers; ceramic materials; metal. Figures 2.3 - 2.6 show images of wafers made of different materials.



Fig. 2.3. Si wafers  
[\*23]

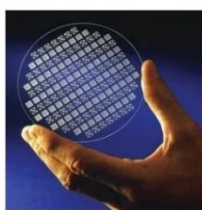


Fig. 2.4. Glass  
wafers [\*18]



Fig. 2.5.  
SiC wafers [\*23]



Fig. 2.6. GaP  
wafers [\*23]

## 2.2. Materials used for deposition

The materials used as substrate are deposited on the wafers used in successive layers, with thicknesses of the order of nanometers to the order of micrometers. The most used materials are:

- silicon and its related materials;
- metals - copper (Cu), aluminum (Al), gold (Au), nickel (Ni), titanium (Ti);
- metallic compounds - titanium nitride (TiN), zinc oxide (ZnO) or titanium-nickel alloys (TiNi);
- ceramic materials - zirconium oxide, silicon nitride, alumina;
- polymers - methyl polymethacrylate (PMMA), polydimethylsiloxane (PDMS) [R4], [P10].

Microdevices can be made of durable, hard but flexible materials and also easy-to-use materials. Carbon-based materials are the latest materials used in the construction of MEMS.

Carbon materials are studied extensively due to their thermal, optical, mechanical and electrical properties, have mechanical strength and ultra-high conductivity [B4], [S5], [K5], [M24], [M18], [M19] [S2] .

## CHAPTER 3. TECHNOLOGIES FOR MANUFACTURING MICRO-ELECTRO-MECHANICAL SYSTEMS

Obtaining and processing micro and nanostructures cannot be achieved without specific unconventional technologies: laser processing technology (Laser Beam Machining - LBM), plasma processing technology (Plasma Machining - PM), ultrasonic machining technology (Ultrasonic Machining - USM ), processing technology with electron beams (Electron Beam Machining - EBM) and ions (Ion Beam Machining - IBM) etc. The expansion of these types of advanced technologies is a response to the main market trends, correlated with the interests in achieving profitability, stability and development. The increased importance of these processing technologies is given by their increasing performance and the superior characteristics that define them.

Geometry modeling is an essential step in the manufacturing process of microelectronics and MEMS devices. The process of transferring an image / geometric pattern from the template (physical or virtual mask) to the plate (usually a silicon plate is used) is called **lithography**.

When this transfer of the image is done with the help of light, the process is called **photolithographic process** (Fig. 3.5). This process is also called **photolithography**.

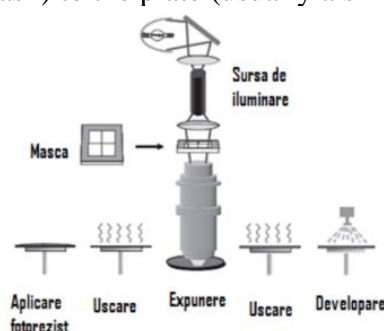


Fig. 3.5. Stages of the photolithography process [M3]

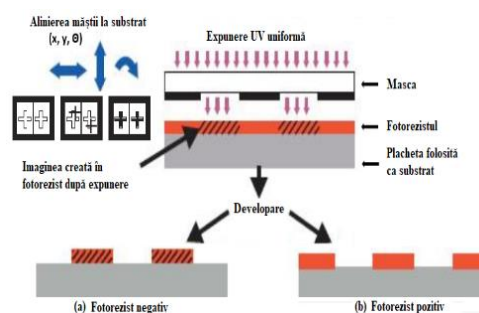


Fig. 3.2. Photoresist layers [adapted after M5]

**Photolithography** is the process that represents the first step in the making of microfabrication, preparing the area for depositing materials. Photolithography allows the protection of certain areas from which it is not desired to remove the material or the protection of some areas from which the material has already been removed. Photolithography is based on photochemical reactions that take place in mixtures of organic substances. These substances are

activated by radiation. The organic substances used are photosensitive polymers called **photoresists** (“photoresist” or “resist”) and allow the erosion of the material located outside the protection zone (Fig. 3.2) [M2], [M20].

## CHAPTER 4. MICROFLUIDICS AND “LAB-ON-A-CHIP” DEVICES

### 4.1. Microfluidics used to separate cells

Microfluidics is a multidisciplinary field, which investigates fluid dynamics on a micrometric scale, with its own phenomena and processes such as: pumping, flow, diffusion, dosing, mixing, etc. **MEMS that use microfluidics in their manufacture are called “lab-on-a-chip” devices** [D1].

Microfluidics is considered to be a technology with enormous potential in terms of conventional equipment and technologies. It is based on many advantages: reduced sample volumes; short reaction time at maximum speed; fast sample processing; high sensitivity; low device costs; device portability [A14].

#### 4.1.1. Classification and number of blood cells

**Blood** is made of two main components: **plasma** and **figurative elements** (Fig. 4.1.). Blood plasma is found in blood in a proportion of 40 - 45%. The figurative elements are represented by the blood cells floating in blood plasma. They are divided into three categories: erythrocytes, leukocytes and platelets.

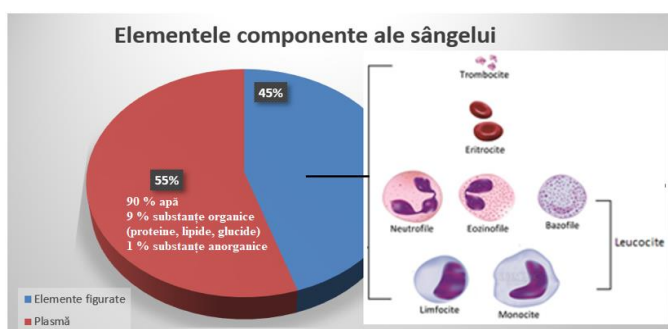


Fig. 4.1. Approximate proportions of blood components

**Leukocytes (white blood cells)** have the **role** of ensuring the protection of the body through **immunity**, by producing antibodies. Due to their size, larger than that of red blood cells and the fact that they can move independently in the bloodstream, they have the ability to quickly reach the site of the wound or infection [M33]. The classification of leukocytes is as follows (Fig. 4.2) [\* 20]:

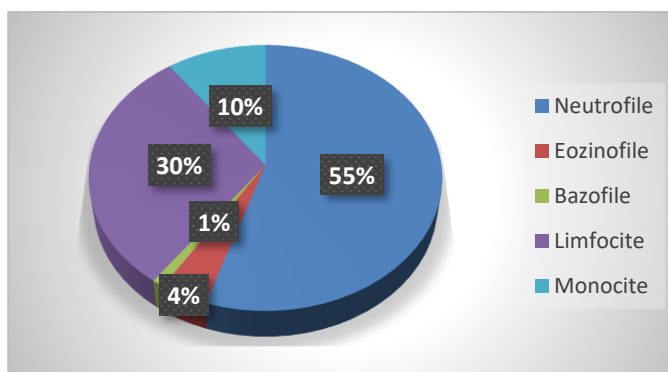


Fig. 4.2. Approximate proportions of leukocytes in the blood

#### 4.1.2. The importance of lymphocytes in the blood

**Lymphocytes** are cells of the immune system, responsible for the body defense reactions to substances considered foreign; they also coordinate the activities of other cells in the immune system. They fight against pathogens: viruses, bacteria, parasites, fungi. Human lymphocytes are divided according to their biological action and the presence of surface markers (on the surface of the cell membrane), in three major classes (populations) [Z4], [\* 20]: Natural Killer Lymphocytes - NK; B lymphocytes; T lymphocytes.

## 4.2. Microfluidic devices construction

As for the materials used in the construction of microfluidics, they are very few. Their history began with the corrosion of the channels directly in silicon. However, given that biological applications involve microscopy, it was wanted to replace this material with one that is transparent and has remarkable optical properties. This material is glass. In addition to the two major advantages it has compared to silicon, it also has resistance [J3]. Over time, other types of materials began to be used. Of these materials, the most common are: polymers: a.) elastomers (eg. PDMS); b.) thermoplastics (eg. PMMA); paper.

## 4.3. Types of microfluidic circuits

Following research, the problem of the intersection angle between the channels was studied. More specifically, microchannels arranged in the form of “Y” and “T” type junctions were studied - two inputs and one output [M30], [\*16]. It was thus found that the angle of  $60^\circ$  is the optimal angle through which the solutions will flow simultaneously (Fig. 4.7.a).

The microfluidic channels through which the cells/solutions circulate may have a serpentine shape (Fig. 4.7.b.) or may be straight. For the introduction of lysis solutions, in most cases side bifurcation channels are used, such as those shown in Fig. 4.7.c.

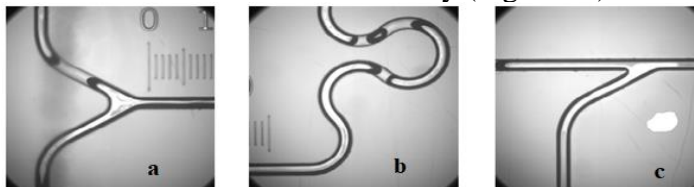


Fig. 4.7. Microfluidic circuits: a.) Straight channels with bifurcation at  $60^\circ$ ; b) coiled microchannels; c) straight microchannels with lateral bifurcation [\*33]

# PART TWO. CONTRIBUTIONS REGARDING THE DEVELOPMENT OF MICRO-ELECTRO-MECHANICAL SYSTEMS WITH APPLICATIONS IN MEDICINE

## CHAPTER 5. OBJECTIVES, RESEARCH DIRECTIONS AND METHODOLOGY ADDRESSED IN THE DOCTORAL THESIS

### 5.1. Synthesis of critical aspects regarding the current state of micro-electro- mechanical systems with applications in medicine

From the critical analysis of the current state of micro-electro-mechanical systems with applications in medicine, certain conclusions with practical applicability emerged, which allowed *the formulation of objectives and the direction of research* in the thesis, as it follows:

1. The current major trend of ultra-miniaturization, present in all areas of manufacturing technologies, which led to the fourth industrial revolution - Industry 4.0, is also manifested in the field of micro-electro-mechanical systems. These have allowed the development of bioMEMS of high technical level, capable of performing certain operations, impossible to perform in the usual way. Some relevant examples are given: taking photos of the digestive tract, replacing endoscopic investigations, nanorobots injected into the body that can be propelled autonomously or remotely controlled, capsules that can be swallowed by patients and enter their bloodstream to perform certain activities of treatment, monitoring, investigation or implants.

2. Micro-electro-mechanical systems have in their structure microsensors, microactuators, microelectronics elements. MEMS applied in medicine can take various forms such as: biomedical transducers, microfluidic devices, medical implants, microsurgical

instruments, etc. The use of microfluidics in the construction of MEMS devices gives them new properties and makes them fall into the special category of bio-devices, called bioMEMS, if they use substances and cells in the human body.

3. Regarding the materials used in the construction of bioMEMS, they are classified as substrate or deposition materials. Highly used silicon in the form of substrate and metals, metallic compounds, ceramic and polymeric materials, as deposition materials, is highlighted. The new trend of development of bioMEMS was also identified, based on carbon materials, represented by graphene and its derivatives, carbon nanowires and nanotubes, using the great advantages offered by these materials, which have high mechanical strength, doubled by low density, associated with exceptional electrical, optical and thermal properties; they can be combined with outstanding results with zinc oxide, titanium dioxide and polymeric materials as deposition materials.

4. The main microtechnologies identified to be used in the manufacture of bioMEMS, in various stages, some even in the thesis, are the following:

- photochemical processing is widely applied, based on the process of photolithography to achieve accuracy; has the advantage of high productivity due to the simultaneous sampling of the material on the entire processed surface, exposed to the process of chemical corrosion after the application of masks, by photoresist substances;

- laser radiation processing (LBM) is used for direct writing of masks, with short wavelength, in the UV range, which ensures a spot diameter in the micrometric or submicrometric range through the ability to create the highest energy density in the industrial field;

- Electron beam processing (EBM) is used for the deposition of thin layers of MEMS and lithography with micrometric and submicrometric precision in two variants, lithography with direct writing by matrix scanning of the material surface and optical lithography by beam design, deflection using electromagnetic lenses;

- ion beam processing (IBM) used for the deposition of thin layer materials (ion plating) in the structure of bioMEMS or sampling of material in the form of two types of dry corrosion, called "Reactive Ion Etching" (RIE) and "Deep Reactive Ion Etching"(DRIE);

- Plasma Enhanced Chemical Vapor Deposition (PECVD) is used for deposition of thin films in the structure of MEMS; thus, thin films of amorphous SiC (A-Si) and vertical graphene (VG) were deposited for use as cell culture substrates for bioMEMS applications;

5. The use of the microfluidics component in micro-electro-mechanical systems, classifies them in the category of microfluidic chips or *lab-on-a-chip* (LOC), which allows them to perform standardized and automated laboratory processes on a micrometric and even nanometric scale; most of this category of devices are in various stages of research and less in marketing - high levels of technological maturity; these devices have the following characteristics:

- LOC devices have diversified components such as: micropumps and microvalves, micromixer, microfilters, chemically functionalized surfaces, electrical control circuits, etc.;

- the advantages of this bioMEMS category, applicable also to the determination of T lymphocytes, compared to the conventional means of analysis, are: the reduction of the sample volume; fast sample processing due to short reaction time; high sensitivity; energy consumed and low costs; portability and reuse of devices, with positive implications for short diagnostic time and prompt treatment. For comparison, the current (conventional) method of leukocyte counting is based on a complex instrument, which must be served by qualified and well-trained personnel. The procedure is at the same time chronophagous, so it has the major disadvantage of delaying proper diagnosis and treatment. Flow cytometry is the standard method for counting T lymphocytes, a method that requires centralized laboratories and trained staff;

- regarding the materials for making microfluidic circuits, hybrid manufacturing technologies that use several materials in the same MEMS are frequently used. These include: a flexible polymer system (polydimethylsiloxane - PDMS) or another polymer, methyl polymethacrylate - PMMA, glass and a rigid polymer (SU-8).

- regarding the shape of the microfluidic circuits, the problem of the intersection angle between the channels was studied, respectively, the arrangement in the form of “Y” and “T” type junctions - two inputs and one output, used for example for the introduction of the sample and substances lysis. There are studies that show that the angles between the junction channels between 45 and 60°, values for which the solutions will flow simultaneously in the microfluidic circuit. The channels can be straight, with connecting radius, twisted or spiral. However, for each device, the functional geometry of the microfluidic channels was established using numerical simulations of the sample flow and the substances used in the analysis in the LOC, which was subsequently validated.

The critical analysis of the relevant aspects of the current stage was the basis for the systemic formulation of the thesis objectives.

## 5.2. Objectives of the doctoral thesis

Following the critical analysis of the current state of micro-electro-mechanical devices with applications in medicine were established: a **main objective (O<sub>p</sub>)** and several **specific objectives (O<sub>si</sub>)**. For their operationalization, these objectives have been formulated as follows:

**O<sub>p</sub>: The main objective of the doctoral thesis is to manufacture for the first time in our country a micro-electro-mechanical system with applications in medicine, designed to count T lymphocytes.**

*This bioMEMS can be used in the early stages of diagnosing serious conditions such as HIV or leukemia.*

Given the complexity of the aspects regarding the manufacture of a bioMEMS for T lymphocyte counting, highlighted in the critical analysis of the current state of the art and research aimed at the practical execution of such a device, two major manufacturing steps were envisaged to achieve the main objective of the microfluidic device: manufacturing the experimental model - ME (industrial research) and manufacturing the prototype - P (experimental development) of the improved device.

In this context, the following definitions were considered regarding the stages of development of the manufacture of the product that is the subject of the doctoral thesis [\*37]:

*Experimental model - system that integrates the component parts, which are in functional form close to or even in operating conditions, according to specifications. This model must demonstrate the functional and operating capabilities of the final system;*

*Prototype - physical model necessary to evaluate the feasibility of manufacturing a product, respectively system, in which its component parts have been integrated.*

Several **specific objectives** (subordinated) to the main objective have been set, grouped in the two major stages, mentioned above, as it follows:

**So1:** Formulation of the general function and the main and secondary functions of the microfluidic device and its corresponding structure;

**So2:** Establishing the geometric shape and dimensions of microfluidic circuits;

**So3:** Establishing the shape and dimensions of the sensors and their arrangement within the microfluidic device;

**So4:** Design of the microfluidic device - experimental model;

**So5:** Design of the technological process of manufacturing the microfluidic device - experimental model;

**So6:** Modeling the technological process of manufacturing the microfluidic device - experimental model;

**So7:** Modeling and simulation of flow in the microfluidic circuits of the microfluidic device - experimental model;

**So8:** Manufacture of the microfluidic device - experimental model;

**So9:** Testing the microfluidic device - experimental model;

**So10:** Identification of non-conformities and their possible causes in the manufacture of the microfluidic device - experimental model;

**So11:** Design of the improved prototype of the microfluidic device and its technological manufacturing process;

**So12:** Modeling the technological process of manufacturing the improved prototype of the microfluidic device;

**So13:** Manufacture of the improved prototype of the microfluidic device;

**So14:** Testing of the improved prototype of the microfluidic device;

**So15:** Integration of the microfluidic device into a portable device and performance of specific reliability tests;

**So16:** Transition from technological maturity level, Technology Readiness Level, TRL 2 - concept phase, to TRL 4 phase, validation of manufacturing technology at laboratory level;

**So17:** Creation of transition conditions to the next levels, TRL 5 which involves the validation of the operation of the entire system of the micro-electro-mechanical device in laboratory operating conditions, similar to the actual operation and TRL 6, validation of operation in a relevant environment, respectively operating conditions close to the real ones.

### **5.3. Research directions and research methodology of the doctoral thesis**

**The major research directions (Di)** that will be acted in the doctoral thesis will be the following, with possible particularizations of some subdirectorates, which will prove important regarding the increase of the performances of the micro-electro-mechanical bio-device, as previously characterized:

**(D1)** modeling the microfluidic device and based on it, studying the hydraulic behavior of microfluidic circuits by modeling and numerical simulation and validating the results obtained experimentally;

**(D2)** modeling the manufacturing process of the microfluidic device and identifying critical steps that could lead to malfunctions, even from the stages of functional and technological design, which are synergistically interconditioned;

**(D3)** experimental research on testing the functionality of the microfluidic device in terms of the behavior of its essential components: sensors, microfluidic circuits with specific elements, counting channels, capture chamber, etc.;

**(D4)** experimental research on the improvement of the micro-electro-mechanical bio-device from the functional point of view and of the manufacturing process, with the validation of the constructive and technological parameters at laboratory level;

**(D5)** experimental research on the specific characteristics of a portable and reusable device that reproduces the actual environmental conditions encountered during manufacture, operation and storage.

The **research methodology** used in the thesis is structured as follows:

- Critical analysis of the current state of micro-electro-mechanical systems, used in medicine (bioMEMS) and approach of an innovative model of bioMEMS, applied to the determination of T lymphocytes in a blood sample;

- Conceptual and detailed design of the microfluidic device for the determination of T - **TRL 2** lymphocytes;

- Establishing recipes for erythrocyte lysis and lysis stopping solutions to determine T lymphocytes in a blood sample;
- Modeling the manufacturing process of a microfluidic device - experimental model for the determination of T lymphocytes;
- Numerical modeling and simulation of flow within the microfluidic device in the following steps: (1) flow of blood sample and erythrocyte lysis substance into the lysis circuit; (2) the flow of the stop substance added to the previous substances in the stop circuit; (3) flow in the counting channel and the capture chamber;
- Experimental validation of modeling and simulation results based on testing the manufactured experimental model;
- Manufacture of a batch of experimental models of the microfluidic device for the determination of T lymphocytes;
- Identifying the non-conformities that appeared during the technological process of manufacturing the experimental model, as well as their causes;
- Eliminating the causes of non-conformities by finding improvement solutions and applying them to the design of the improved prototype of the microfluidic device for determining T lymphocytes and its technological manufacturing process;
- Manufacture of the improved prototype of the microfluidic device and its testing in order to validate the operation in laboratory conditions, as well as the validation of its manufacturing technology in the laboratory - **TRL 4**;
- Integrate the microfluidic device into a portable device and subject it to laboratory tests specific to such devices, under conditions *similar* to those encountered in a real environment - **TRL 5 or close to it - TRL 6**.

## CHAPTER 6. RESEARCH ON THE DESIGN, MODELING AND SIMULATION OF A MICRO-ELECTRO-MECHANICAL DEVICE FOR DETERMINING T LYMPHOCYTES, EXPERIMENTAL MODEL

### 6.1. General data

The MEMS micro-electro-mechanical device is a device for detecting the number of “**Total CD3 + lymphocytes**” (“cluster of differentiation” 3 - CD3 +), “**CD4+ T helper lymphocytes**” and “**CD8 + suppressor / cytotoxic T lymphocytes**”. T lymphocytes have various categories of receptors on their membrane surface. CD3 +, CD4 + and CD8 + are the subcategories of receptors for antigen recognition [M16], [M20], [M21], [M22].

### 6.2. Establishing the functions and the functional structure of the product

In order to determine the fulfillment of all the functional requirements of such a microfluidic device, its structure was designed from the following specific blocks (Fig. 6.1):

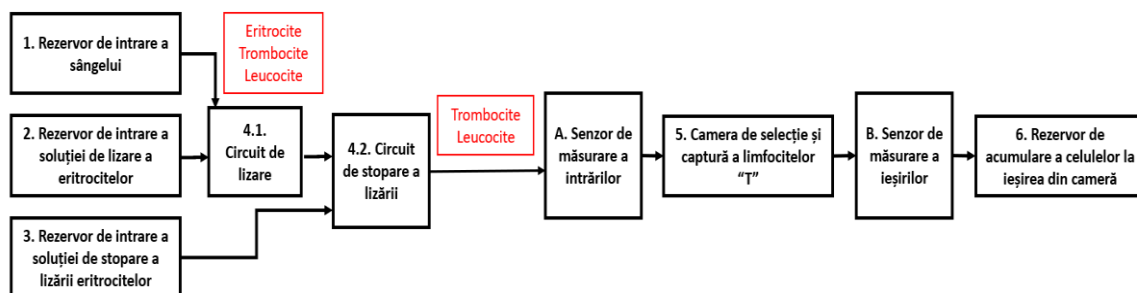


Fig. 6.1. Scheme of the microfluidic device for the determination of T lymphocytes

The microstructured microfluidic device has been designed to be of increased sensitivity and specificity to other microfluidic devices for similar purposes. It is made of four specific elements:

1. leukocyte enrichment segment, consisting of two modules:
  - a. erythrocyte lysis module;
  - b. the module for stopping the lysis;
2. the microchannel segment;
3. leukocyte capture segment;
4. leukocyte counting segment, consisting of:
  - A. Input measurement sensor;
  - B. Output measurement sensor.

A capture chamber that allows the specific selection of CD3+, CD4+ and CD8+ lymphocytes, using specific anti-CD3+, anti-CD4+ and anti-CD8+ antibodies has been designed. The antibodies will be immobilized by the pillars in the lymphocyte capture chamber. Thus, the two electrochemical sensors will be placed before entering the capture chamber and at the exit of the camera. They will count one by one the leukocytes that enter the room and those that leave the room. The lymphocyte population to be quantified will remain trapped in the capture chamber. The difference between the number of entries and the number of exits from the room will represent the number of CD3+, CD4+ or CD8+ lymphocytes.

### 6.3. Technological data obtained in the laboratory

For erythrocyte lysis, the commercial product 10X RBC Lysis Buffer (Multi-species) from ThermoFisher Scientific was used, which is specially formulated for optimal lysis of erythrocytes in single-cell peripheral blood suspensions and hematopoietic tissues, such as the spleen. 10X RBC Lysis Buffer (Multi-species) contains ammonium chloride, which lyses red blood cells with minimal effect on lymphocytes [\*38]. To stop lysis, salt phosphate buffer pH 7,1 is pumped onto the corresponding microchannel.

The optimal ratio between the blood sample, the lysis solution and the stopping solution was studied. The optimal ratio of blood solution: lysis was found to be 1:12. Under these conditions, the blood flow was set at 5  $\mu\text{l} / \text{min}$  and the lysis solution flow was set at 60  $\mu\text{l} / \text{min}$ , so that the time spent in the lysis section did not exceed 6 seconds. For the lysis stop section, the ratio of the mixture in the lysis section to the lysis stop solution is recommended to be 1: 6, so that it takes at least 30 seconds for the stop solution to mix with the lysed blood and allows complete lysis of erythrocytes.

### 6.4. Establishing the shape of microfluidic pathways

To establish the dimensions of the fluid channels, a presimulation of the main elements was performed with the help of the ANSYS® FLUENT program, dedicated exclusively to CFD (Computational Fluid Dynamics) modeling.

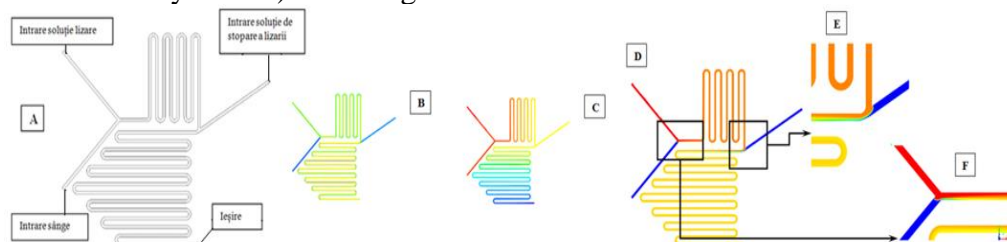


Fig. 6.2. Modeling and simulation of flow in the microfluidic system: A) Module of the erythrocyte lysis circuit coupled with the lysis stop circuit; B) Pressure distribution; C) Gear distribution; D) Representation of the dissemination process; E), F) Detail of the diffusion process [M16]

### 6.5. Design of the micro-electro-mechanical device, experimental model

The stages of the technological flow for the manufacture of the micro-electro-mechanical device, experimental model, include a succession of specific material deposits. This sequence of deposits is shown in Fig. 6.4. A silicon wafer is used (1) on the surface of which a layer of silicon oxide (2) will be deposited. A layer of photoresist (3) will be spread over it, used as a sacrificial layer to expose the first mask over which a layer of titanium-gold will be deposited (4). This is followed by the process of cleaning inactive areas, a process called lift-off (5). A new photoresist layer (6) will be deposited over which the silver used in the construction of the reference electrodes will be deposited. Then another lift-off process will take place (7). The last layer deposited will be the photoresist SU-8 2050, used for the construction of the microfluidic part (flow circuits). Finally, a PDMS cover (10) will be attached to the device. The intermediate material with which these deposits are made is the photoresist.

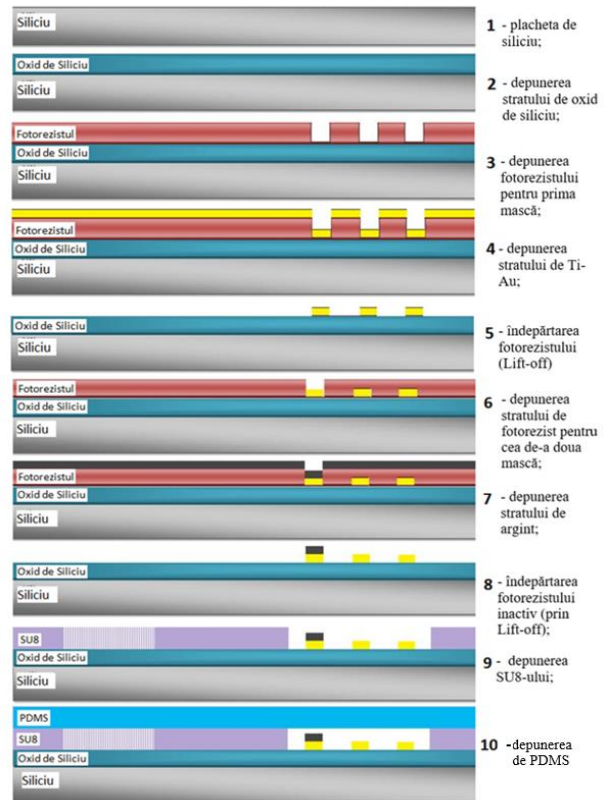


Fig. 6.4. The stages of the technological flow [M16]

- **Design of the first mask**

The first mask (M1) is made of titanium-gold and contains the two sensors for measuring inputs and outputs, as well as the reference edges of the device. In order to be able to differentiate the masks from each other, it is recommended that each mask to be made using a different color. The yellow color was used for this mask (Fig. 6.15). Each wafer contains four microfluidic devices.

- **Design of the second mask**

The second projected mask (M2) (represented with red in Fig. 6.20) is intended for the layer on which the silver will be deposited. It is necessary to deposit silver on the surface of a single electrode, namely the reference one.

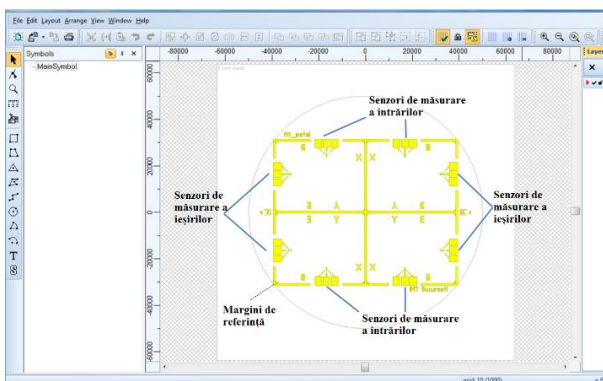


Fig. 6.15. The first specific mask of the device

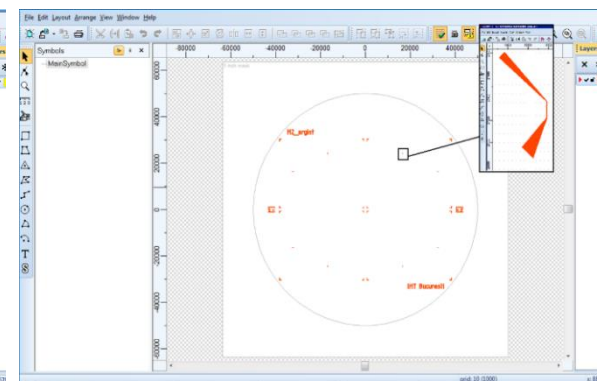


Fig. 6.20. Designing the second mask

- **Design of the third mask (M3)**

This mask (M3) is made for the deposition of negative photoresist (SU-8), used in the definition of microfluidic channels. The image of the third designed mask can be seen in Fig. 6.22. It comprises four nanoports: A1. for blood; A2. for the solution of lysing erythrocytes in the blood; A3. for the lysis stop solution; A4. for storing the remaining cells; as well as B. microchannels; C. selection and capture chamber.

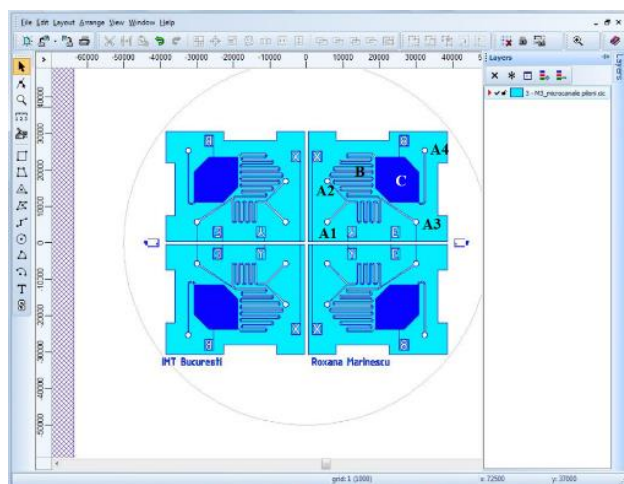


Fig. 6.22. Design of the third mask

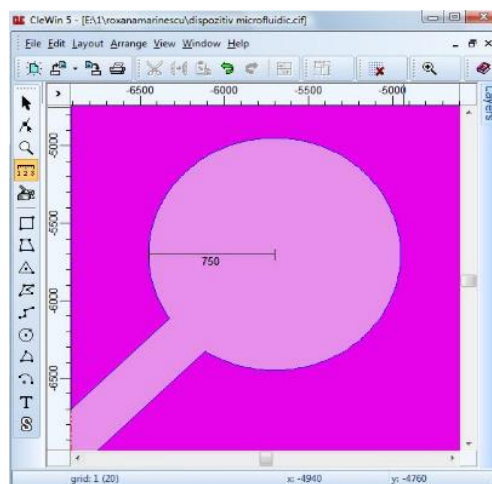


Fig. 6.24. Nanoports design

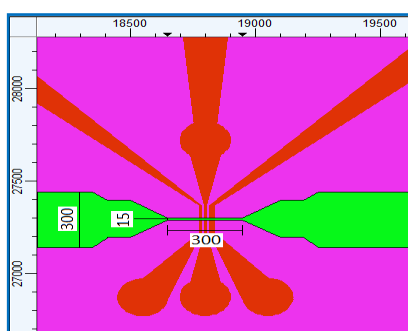


Fig. 6.25. Design of the counting microchannel in the sensor area

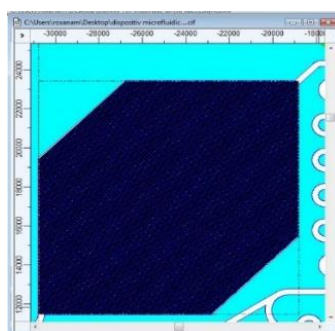


Fig. 6.26. Selection and capture chamber

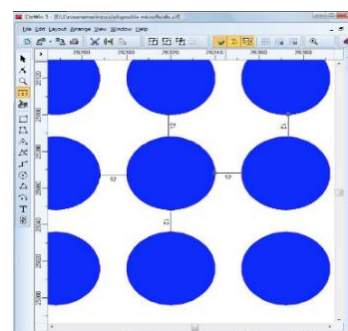


Fig. 6.28. Distance between pillars

The four nanoports represented A1, A2, A3, A4 in Fig. 6.20 have a radius of  $750 \mu\text{m}$  (Fig. 6.24). The width of the microchannels is  $300 \mu\text{m}$ . The microfluidic channel narrows to  $15 \mu\text{m}$  in the area of the electrochemical sensors for counting the inputs and outputs, over a distance of  $300 \mu\text{m}$ , so that the cells enter one by one, to avoid conglomeration, respectively counting errors. This detail can be seen in Fig. 6.25. The selection and capture chamber has a hexagonal shape and is represented by the blue color in Fig. 6.26. The pillars have a diameter of  $40 \mu\text{m}$  (Fig. 6.27) and a distance of  $12 \mu\text{m}$  between them that allows the passage of lymphocytes (Fig. 6.28), being projected 54230 pillars inside the selection and capture chamber.

- **Masks, alignment and exposure**

The manufacture of photolithographic masks begins with the design of geometries. The masks contain the geometries that will be transferred to the photoresistor displayed on the plate. The file created in the specialized program CleWin5 is used to generate transparent or opaque areas on the mask.

In order to obtain a correct alignment of the masks, it is necessary to manufacture alignment marks that are transferred to the substrate. With the help of alignment marks, the masks will be relatively oriented to each other in the manufacturing of the microfluidic device. In Fig. 6.33. the image of the three masks is observed when designing them, while they are being designed in the overlapping phase.

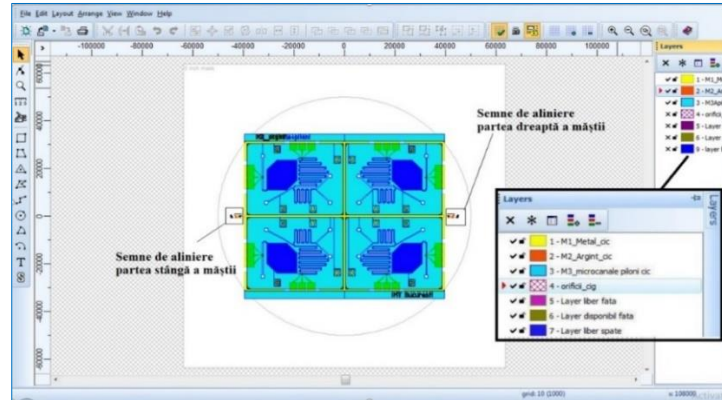


Fig. 6.33. The three overlapping masks

### 6.6. Modeling the manufacturing process of the micro-electro-mechanical device, experimental model

Using the “SEMulator3D™” program, 3D models were generated for the modules that make up the biochip for the determination of T lymphocytes. Going through the modeling steps of the manufacturing process presented above, the configuration of the devices with the tanks (through which the solutions are introduced) attached will look according to Figures 6.37 and 6.52.

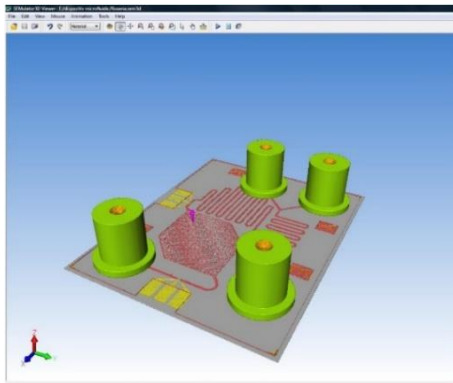


Fig. 6.37. Modeling the tanks for introduction of substances into microfluidic circuits

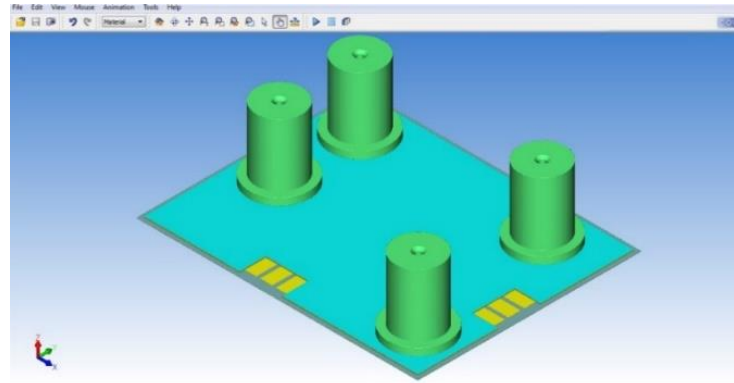


Fig. 6.52. Microfluidic device configuration after modeling the manufacturing steps

Using SEMulator 3D, the correctness of the design in order to manufacture the device was demonstrated and the parameters established in the design phase for the realization of the T lymphocyte detection device were verified, which define the expected results to be obtained.

With the help of this program it is proved that the sequence of standard steps is in accordance with the manufacturing process of the intended device, made with the desired characteristics.

### 6.7. Computer modeling and simulation of microfluidic flow in the micro-electro-mechanical device, experimental model

The dedicated Comsol Multiphysics finite element modeling software [C17] was used and then the modules, *Fluid Flow*, *Single Phase Flow* and *Laminar Flow* were successively selected for modeling and simulating the flow of substances used in the microfluidic device. The input data presented above are reproduced in Table 6.3 [G5].

Table 6.3. Input data for performing the microfluidic simulation

Flow ratios	
Blood	50 $\mu\text{l}/\text{min}$
Lysis solution	1600 $\mu\text{l}/\text{min}$
Lysis stop solution	265 $\mu\text{l}/\text{min}$

The parameterization of the model geometry after the iterative constructive and dimensional optimization is presented in Table 6.4 [G5]. With the help of these parameters, the geometry was modeled in Comsol, according to Fig. 6.55.

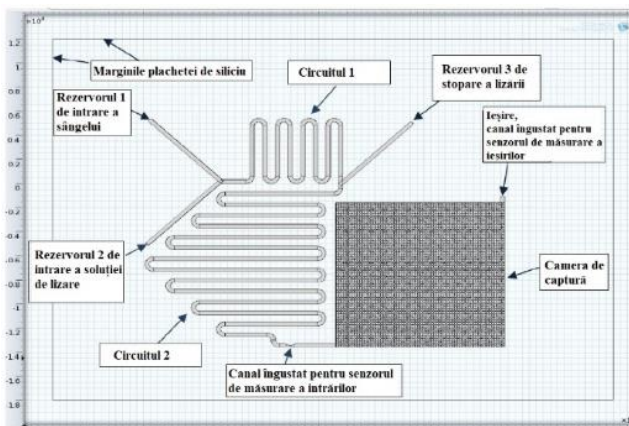


Fig. 6.55. Creating the geometry of the microfluidic device with the design data [G5]

Table 6.4. Simulation parameters [G5]

Parameters			
Name	Expression	Value	Description
I1c	40000	40000.0	chip length
I2c	30000	30000.0	chip width
a	300	300	channel width
I1	7300	7300	channel 1 length
I2	1800	1800	channel 2 length
rrac	300	300	curve radius
I3	4200	4200	channel 3 length
d1	1000	1000	distance from circuits
I4	7800	7800	channel 4 length
I5	6600	6600	channel 5 length
I6	8400	8400	channel 6 length
I7	10200	10200.0	channel 7 length
I8	11700	11700.0	channel 8 length
I9	3000	3000	channel 9 length
I10	500	500	channel 10 length
b	300/4	75	chamfer 1 length
I11	200	200	chamfered channel length
c	$(a-2*b-d)/2$	67.5	chamfer 2 length
d	15	15	counting channel diameter
I12	100	100	counting channel length
I13	3000	3000	input length in capture chamber
lcap	12044	12040.0	capture chamber side length
distp	12	12	distance between pylons
rp	176/2	88	pylon radius
xch	-12000	-12000.0	x chip
y ch	12000-30000	-18000.0	y chip

The simulation of the flow rate of the fluid mixture is presented in Fig. 6.57 [G5]

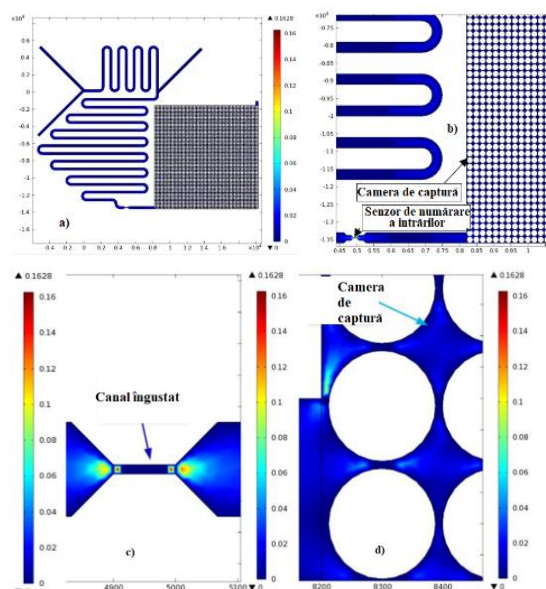


Fig. 6.57. Flow rate variation [m / s], a) overview, b) circuit detail, c) counting channel, d) enlarged view of the selection and capture chamber [G5]

The modeling and simulation of microfluidic flows in Comsol Multiphysics was performed. Finite element modeling determined the optimized geometry of the flow circuit of the "lab-on-a chip" device on a silicon wafer, for counting the types of T lymphocytes by electrochemical sensors. The model developed in Comsol Multiphysics was validated by post-manufacturing testing, meeting the travel time conditions of the blood sample and the reactive substances in the flow circuits, necessary for a proper analysis. The reusable device has the advantage of providing fast and reliable test results of a low-volume blood sample.

## CHAPTER 7. MANUFACTURE OF A MICRO-ELECTRO-MECHANICAL DEVICE, EXPERIMENTAL MODEL

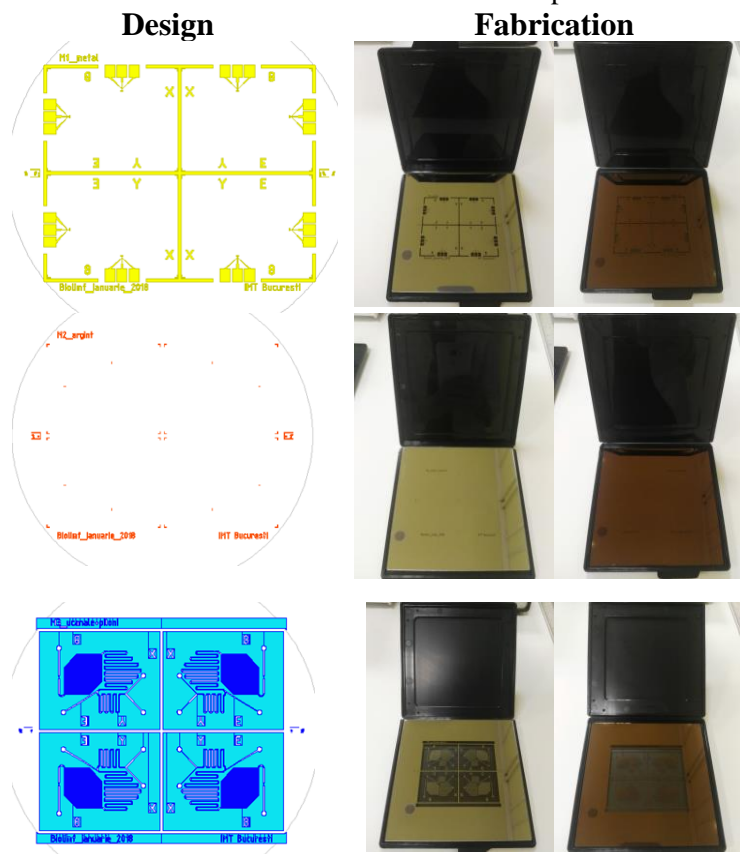
Tabele 7.1. The three masks of the microfluidic device, experimental model

**Mask 1 (M1)** - used for the deposition of the layer composed of titanium and gold, on which the leukocyte counting segment was designed, consisting of the two sensors: the electrochemical sensor for counting the inputs and the electrochemical sensor for counting the outputs;

**Mask 2 (M2)** - used for depositing silver; silver is deposited on the surface of only one electrode of each sensor: the reference electrode;

**Mask 3 (M3)** - used for the deposition of the photoresist SU-8, in which were made by photolithography, microfluidic channels, holes for the introduction of solutions used in the lab-on-a-chip analysis process, as well as the selection and capture chamber.

Table 7.1 shows the three masks (front view and back view - right side) made with the DWL 66-fs laser writing equipment in correspondence with the drawing designed in CleWin program for each mask (left).



### 7.2. The actual manufacture of the device, experimental model

**A batch of five silicon wafers was used to make the device. Four microfluidic devices were placed on each of these five wafers. Thus, the manufacturing batch consisted of 20 products.**

The actual execution of the microfluidic platform takes place according to the technological flow previously established with the following steps, presented below.

#### 7.2.1. Silicon wafer used as substrate

The manufacture of the microfluidic bio-device was carried out starting with the choice of a substrate. For this device, the monocrystalline silicon wafer with a diameter of 100 mm was chosen as substrate.

#### 7.2.2. Silicon oxide deposition

The first step in making the device is to grow a thin layer of silicon oxide on the surface of the wafer. The oxide layer that has been deposited (Fig. 7.5) acts as an insulating layer between the silicon and the metal layer to be deposited. It is a barrier to the penetration of

impurities into the base material [A12]. After the deposition of the oxidation layer, an intermediate step was performed to verify the deposited thickness (Fig. 7.6) with the help of NanoCalc-XR equipment (Ocean Optics, Germany) [\*9], [\*34].

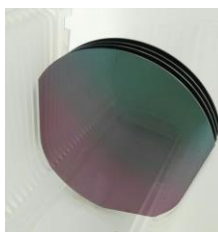


Fig. 7.5. Silicon oxide deposited on wafers

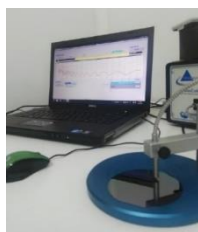


Fig. 7.6. NanoCalc-XR equipment [M20]



Fig. 7.8. LOR 10B photoresist deposited on the wafer



Fig. 7.9. Spinner Suss MicroTec equipment



Fig. 7.10. Thermal treatment on plate equipment

### 7.2.3. Photolithography for the first mask

After increasing the silicon oxide layer, the photoresist was deposited on the entire surface of the wafer. It is used to determine the geometric shape of the material to be deposited over silicon [M23]. The deposition of the photoresistor goes through the three stages: **display** → **exposure** → **development**.

The first layer of photoresist to be applied to the silicon wafers is called LOR 10B and is a positive photoresist used as an auxiliary solution to the subsequent lift-off process. The photoresist was deposited on the wafers by dripping (Fig. 7.8). It was spread on the entire surface of the wafers by centrifugation using the Suss MicroTec equipment (Germany) called “spinner” (Fig. 7.9) [\*9], [\*27], choosing a rotation speed of 3000 rpm and a time of 30 - 40 s. A layer with a thickness of 1  $\mu\text{m}$  resulted. To solidify the resin, the silicon wafers with the deposited photoresist layer were heat treated on a preheated plate. For pre-baking, the plates are kept for 3 minutes at 150 °C on the Selecta Combiplac plate (Barcelona) [\*28] (Fig. 7.10). Then, each plate was exposed to ultraviolet (UV) light for 50 s. Next, a second layer of positive photoresist, called HPR 504, was deposited in the same way: displayed using the Suss MicroTec spinner [\*27] at 3000 rpm and a time of 30 - 40 s. After the deposition of the photoresist HPR 504, the wafers were placed on a hot plate for a 1 min at 90 °C treatment.

For the transfer of the image from the mask to the surface of the substrate, with ultraviolet (UV) light, the equipment MA6 / BA6 (Suss MicroTec, Germany) [\*27] was used, which is an equipment for double alignment (front / back) of the plate. The mask is fixed in the equipment with vacuum (Fig. 7.14. a, b), and under the mask is fixed the plate (Fig. 7.15. a, b).



Fig. 7.14. a) orientation and b) fixing the mask in the MA6 / BA6 equipment



Fig. 7.15. a) orientation and b) fixing the wafer in the MA6 / BA6 equipment

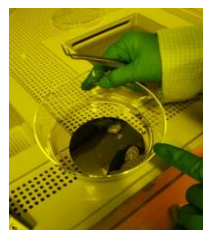


Fig. 7.16. Wafer development in HPRD 402 solution



Fig. 7.17. Rinsing the wafer with deionized water

The development solution used to remove the acidic components of the photoresist was acetone together with the substance HPRD 402. This mixture removes the photoresist layer that was exposed, leaving the transposed image on the first mask. After each wafer was placed in

solution for 15-30 seconds (Fig. 7.16), it was rinsed with deionized water (Fig. 7.17) [M16]. After rinsing the wafer abundantly with deionized water, it was dried with nitrogen to remove most of the water and then dried with a centrifuge [\*9] to remove any traces of solution or water remaining on the surface.

- **Intermediate inspection**

In order to see the results obtained and whether the photoresist was properly removed from the exposed areas, the intermediate inspection was performed, using a Leica optical microscope, model DM LM (Leica Microsystems, Germany) from IMT Bucharest [\*9], [\*29], which has lenses from x5 to x100.

In case of improper development, where the photoresist was partially removed, the wafers were again put in the developing solution for a few seconds to remove the remained photoresist. After the second intermediate inspection, it was found that all developments were conform. Thus, it is possible to proceed to the next step, that of depositing the titanium-gold layer.

#### 7.2.4. Deposition of the titanium-gold layer

A 30 - 300 nm Ti-Au layer was deposited. The titanium layer is deposited between the silicon (oxidized) substrate and the gold layer to ensure adhesion. This titanium-gold deposition was made on the entire surface of the plate and was made immediately after the photolithography process to avoid contamination. The next lift-off process limits the deposition thickness of the metal layers. After removing the photoresist, the metal remained only in the windows exposed in the previous step [M16]. The equipment on which the vacuum is deposited is called Neva-EVD 500A (Neva, Japan) (Fig. 7.19)



Fig. 7.19. Neva EVD 500 A equipment  
a) overview of the equipment;  
b) control panel

#### 7.2.5. Lift-off removal of the photoresist for the first mask

After depositing the Ti-Au layer, the lift-off process follows. The wafers are immersed in a vessel containing acetone (Fig. 7.20) at room temperature and shaken until the photoresist comes off together with the metal deposited on it. This acetone solution should be changed regularly to avoid re-deposition of detached metal particles on the electrodes, as they may adhere to the wafer [M16].

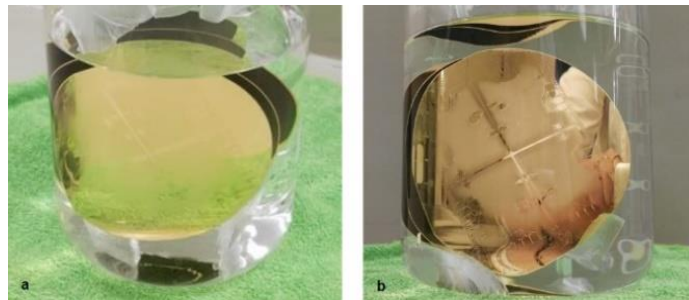


Fig. 7.20. a) Introduction of wafers in acetone solution for the lift-off process; b) activating the gold layer removal process

The fact that the gold deposits over the silicon oxide layer were made successfully is observed both with the eye and with x5 and x10 resolution images, made with Leica DM LM optical microscope (Leica Microsystems, Germany) ( Fig. 7.21) [\*9], [\*29]. In Fig. 7.22 images of the input sensors of a device can be seen.

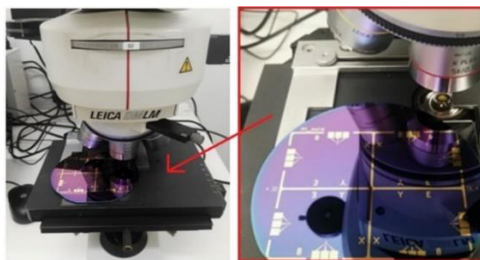


Fig. 7.21. Microscopic inspection of the wafer after making the first mask

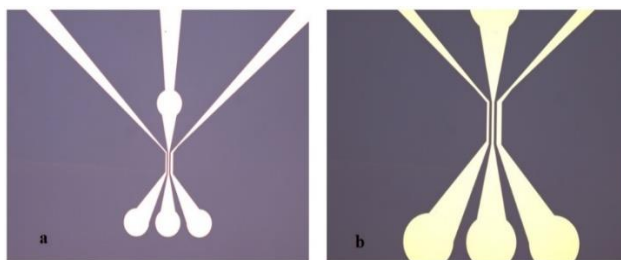


Fig. 7.22. Input measuring sensor examined under the Leica DM LM microscope in dimensions a) x5 and b) x10

### 7.2.6. Photolithography process for the second mask

The deposition of the photoresist for the second mask was done using the same two types of positive photoresist LOR 10B and HPR 504, using the same equipment used to make the first mask. The only difference is that another mask (M2) is used [M16].

### 7.2.7. Deposition of the silver layer

A 100 nm thick silver layer was deposited on the entire surface of the wafer, using the same equipment used for gold deposition, Neva-EVD 500A equipment. The deposition of the silver layer is done to functionalize the reference electrode (RE). Only this electrode will remain covered with silver after the lift-off process [M16].

### 7.2.8. Removal of the photoresist by lift-off for the second mask

The definitization of the reference electrodes (RE) was done by lift-off. The solution used for the lift-off process was acetone. The wafers were allowed to soak in acetone for about a whole day, so that the photoresist came off together with the unwanted metal on their surface. After the lift-off, the silver must remain deposited on a single electrode [M16]. In Fig. 7.24, are presented several phases of the silver removal process.

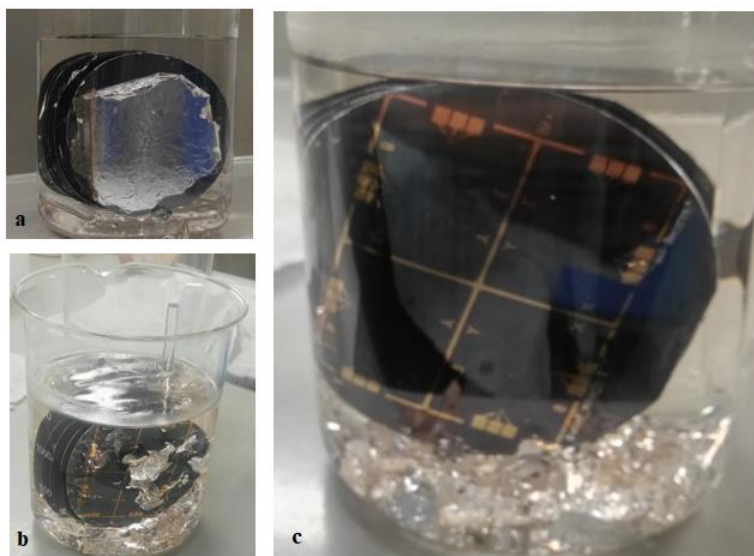


Fig. 7.24. Lift-off silver removal. a) the detachment of the silver starts from the edges; b) central detachment of silver; c) total detachment of silver

The intermediate inspection consisted of checking the deposits using Leica DM LM optical microscope. This was done individually for each wafer. Each of them contains four devices. Following the intermediate inspection, it was found that 11 out of 20 devices are conformable. If one of the sensors was conformable and the second was non-conformable, then the device will not be used because it is not functional without one of the sensors. Only if both sensors are conformable, the device can be used. There have also been cases in which a piece of silver was detached from areas of no interest, so that the sensor was functional. The selection of the functional sensors is presented in Table 7.9.

Table 7.9. Conformable / non-conformable electrochemical sensors of the five wafers

	Wafer 1		Wafer 2		Wafer 3		Wafer 4		Wafer 5	
	Input sensor	Output sensor	Input sensor	Output sensor	Input sensor	Output sensor	Input sensor	Output sensor	Input sensor	Output sensor
Device 1:	DA	DA	NU	NU	DA	DA	DA	DA	NU	DA
Device 2:	DA	DA	NU	NU	DA	NU	NU	DA	DA	DA
Device 3:	NU	DA	NU	NU	DA	NU	DA	DA	DA	DA
Device 4:	DA	DA	NU	NU	DA	DA	DA	DA	DA	DA
Functional devices	3		0		2		3		3	
Total of functional devices	11/20 conformable device									

Symbols:

DA - conformable sensor;

NU - non-conformable sensor.

Conformable devices have the answer "DA".

Non-conformable devices have the answer „NU”.

Nonconformities can have various causes: platelet contamination; high humidity in the equipment room; the electrode deposition area is too small. Regarding the elimination of these causes, the dimensions of the reference electrodes were changed and the deposits were made at a controlled humidity level in the room.

- **Silver chlorination**

After the silver deposition, an intermediate stage of the technological process of chlorination was performed, which had the role of minimizing the contact resistance of the electrode. Silver chlorination is a necessary step in creating a stable electrode. Silver can be electrochemically chlorinated in chlorine solution. The solution of KCl (potassium chloride) is widely used. An alternative method is non-electric chlorination with FeCl<sub>3</sub>.

### 7.2.9. Photolithography process for the third mask

The third mask was used to make the microfluidics part: the microchannels and pylons in the selection and capture chamber. These will be made of SU-8-2050 [M23]. The SU-8 photoresistor is deposited by following the steps shown in Figs. 7.26 [M23], [P7].

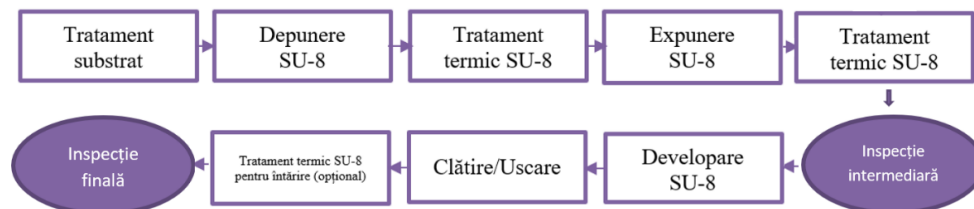


Fig. 7.26. The stages of the technological process of modeling microfluidic circuits using SU-8 photoresist

After the previous silver lift-off process, the wafer were dehydrated in an oven at 100 °C for about 30 minutes - 1 hour. After that, each plate was fixed on the Suss MicroTec spinner [\*9] to display the SU-8 negative photoresist on its entire surface. The manufacture of microchannels and pylons from the selection and capture chamber was chosen from SU-8, because it has an excellent chemical resistance, high transparency, is biocompatible and has a

strong adhesion. A thickness of the photoresist SU-8 of 50  $\mu\text{m}$  was deposited in order to be able to manufacture the channels and pylons in the selection and capture chamber. To obtain this size, the spinner speed was adjusted to 4000 rpm.

After deposition of the photoresist SU-8, the platelets were placed on the hob for heat treatment at 65 °C for 3 min and 6 minutes at 45 °C [M16].

In the next technological stage, the alignment and exposure of the third mask (M3) to the MA6 / BA 6 equipment (Suss MicroTec) was performed.

A heat treatment was performed on the plate to harden the photoresist (2 min at 65 °C / 7 min at 45 °C). After the heat treatment, the development was performed in acetone solution and HPRD 402 which lasted 1 min 30 s  $\pm$  10 s. After the development took place, followed by the drying of the platelets, an intermediate inspection was performed.

The intermediate inspection was performed with the Leica DM LM optical microscope [\* 9], [\*29]. Following the inspection, it was found that the photoresist SU-8 did not adhere to one of the wafers (wafer number 3). In Fig. 7.29 an image containing nonconformities is presented. It was decided to continue the process with a batch of three wafers that were conformable. For the fourth wafer, it was necessary to remove the SU-8 photoresist and resume the process.

Hardening the photoresist by heat treatment at a high level plays an important role. First, if there are deposition defects that are generated in the silicon layer, they will be filled with photoresist. Moreover, through this heat treatment to harden the layer, the adhesion of the photoresist to silicon increases [A11]. Both the microchannel next to the sensors and the pillars in the selection and capture chamber were checked. Table 7.10 presents images of the microchannel, made with the Leica DM LM optical microscope (Leica Microsystems, Germany) [\* 9], [\* 29], (Fig. 7.33) at magnification scales of x5 and x10.

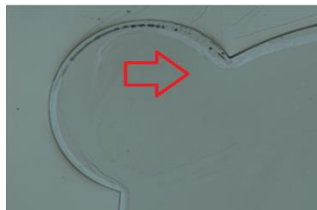


Fig. 7.29. Image taken at size x5 of the non-conformable solution inlet tank

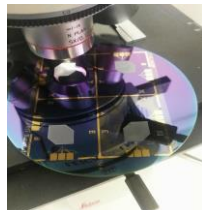
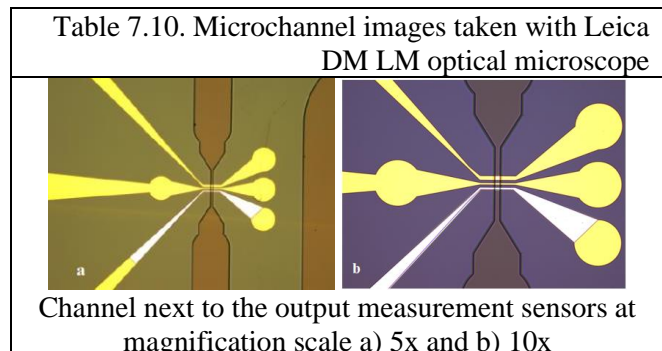


Fig. 7.33. Final inspection after making all the masks



Before the PDMS deposition, the wafers were cut into structures in order to be able to separate the microfluidic devices. Each wafer is cut individually. In order to be cut, the wafer is fixed with a support, where it will be glued exactly in the middle. The cutting operation is performed using the equipment DAD322 - Disco Automatic Dicing Saw [\*17]. After the wafer was fixed on the support (Fig. 7.35.a), it was inserted into the DAD 322 equipment (Fig. 7.35.b.).

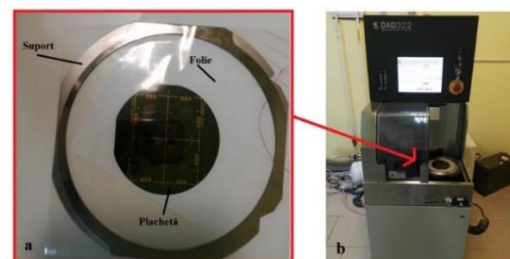


Fig. 7.35. a) fixing the wafer in the holder and b) inserting the holder in the DAD 322 equipment

The last step before detaching the cut devices from the backing foil was UV exposure. The insert foil was inserted into the ultraviolet oven model CL-1000 Ultraviolet Crosslinker, produced by UVP, LLC - USA [\*17].

### 7.2.10. Polydimethylsiloxane cover deposition

The device was encapsulated with a layer of polydimethylsiloxane (PDMS), without covering the electrical contacts. The concentration used for the PDMS mixture differs depending on the desired layer thickness. For a thin layer of PDMS (1-2 mm) 0,7ml of Silicone Elastomer Curing Agent and 7ml of Silicone Elastomer - Base were mixed. For a greater thickness ( $\approx 5$ mm), concentrations of 20 ml - 2 ml of solution were mixed.

Silanization of the mold is performed to prevent the PDMS from sticking to the mold. The release agent (solution) is vaporized. Silanization takes place in a closed enclosure, the substance was placed in the same box in which the silicon wafer is kept, used as a support for pouring the PDMS. The box was left for about an hour at room temperature (Fig. 7.41). At the end of this hour, the PDMS was poured into the special device over the silicon wafer used as a support (Fig. 7.42). Thus, the obtained PDMS layer was uniform (Fig. 7.43). For surface functionalization, plasma treatment was required to attach the PDMS cap to the microfluidic device. The plasma equipment used is a "Reactive Ion Etching - RIE" type, called Plasma Etcher - Etchlab 200 from Sentech (Fig. 7.45).



Fig. 7.41. The silanization process



Fig. 7.42. Pouring the PDMS into the holder



Fig. 7.43. Obtaining the uniform layer of PDMS



Fig. 7.45. Attaching the PDMS cover

An inspection of the pillars from the capture and selection chamber was made using an electronically scanning microscope, Nova NanoSEM 630, manufactured by FEI Company, USA, from IMT Bucharest (Fig. 7.46) [\*17]. To capture these images, a sectioned device was used (Fig. 7.47). The device chosen was one of those whose silver deposit was non-conformable. This was a device to which no PDMS cover was attached. In Fig. 7.49 - 7.50 two images at different reference sizes ( $200\ \mu\text{m}$  and  $50\ \mu\text{m}$ ) of the pillars in the selection and capture chamber are rendered.



Fig. 7.46. Nova NanoSEM 630 equipment

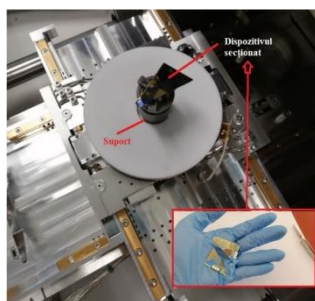


Fig. 7.47. Positioning the sample on the support

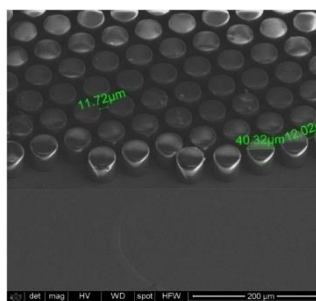


Fig. 7.49. SEM image obtained at the reference size  $200\ \mu\text{m}$

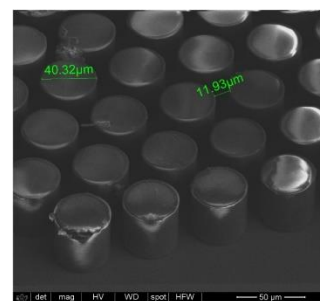


Fig. 7.50. SEM image obtained at the reference size  $50\ \mu\text{m}$

From the SEM images it resulted that the pillars made of photoresist were in terms of dimensions and arrangement in the selection and capture chamber (reciprocal position).

## CHAPTER 8. DEVICE TESTING, EXPERIMENTAL MODEL

## 8.1. Testing methodology

A methodology for testing a microfluidic device was developed, framed in the holistic process of its manufacture - design, modeling, simulation, execution, testing, delivery. The general scheme of the steps to be monitored is presented in Fig. 8.1.

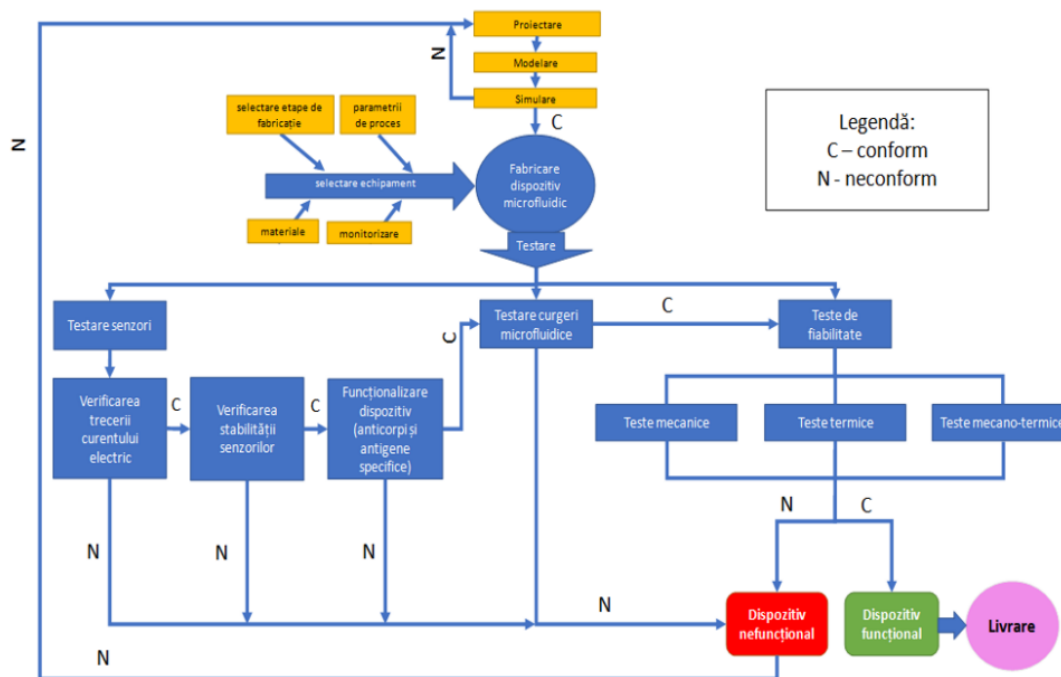


Fig. 8.1. The stages of the testing methodology of a microfluidic device

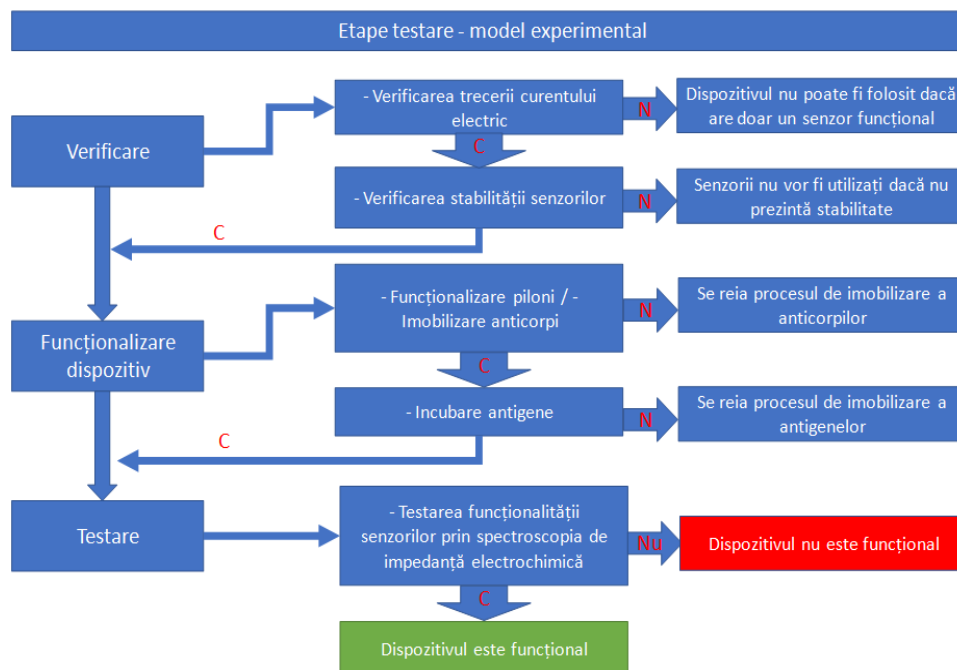
To achieve a microfluidic device, the classic design-modeling-simulation stages must be completed. The modeling and simulation results are to be validated by the results obtained from the post-manufacturing test.

Specific equipment will be used for manufacturing, for which the manufacturing stages, working parameters and materials are selected. Manufacturing processes include quality inspection steps, performed by testing functional parameters.

The tests take place in successive stages: (1) testing the sensors (to check if they are conductive, (2) testing the stability of the sensors (in case of instability, at each test, the sensors will give different results); (3) functionalization tests of the device, by binding of antibodies and incubation of antigens, to capture the cells that are the subject of the lab-on-a-chip device, only if all three steps lead to compliant results, proceed to the following steps: microfluidic flow testing (tests shall be performed to verify the construction of microchannels, which ensure fluid flow). If these tests have compliant results, proceed to the final test: (5) testing the reliability of the device in operating conditions close to those encountered in a without these reliability tests, no device can be delivered (launched on the market).

In Fig. 8.1, if the results are conformable, they are marked with "C", and the non-conformable results with "N". If the result of a stage is "N", the device is not functional and returns to the previous stages of the holistic manufacturing process.

In order to test the manufactured device and to demonstrate its functionality, several steps were taken. These tests were performed within the IMT before gluing the PDMS cover to the device. The logic diagram of the test steps for the micro-electro-mechanical device, experimental model, is presented in Fig. 8.2.



Legend: C – conformable; N – non-conformable

Fig. 8.2. Stages of testing the micro-electro-mechanical device, experimental model

In a first phase, the “Verification” stage takes place, during which the lab-on-a-chip devices with functional sensors were selected, which allowed the current to pass. It is also specified that the device cannot be used if it has only one functional sensor.

Then, the stability of the electrochemical sensors was checked. If the sensors do not have stability - they give different results for each test - they cannot be used, being marked with "N".

If the answers were in accordance (marked with "C") it can be proceed to the next steps of operating the device. Antibodies were attached and subsequently different concentrations of CD3+, CD4+, CD8+ antigens were incubated [M27]. If incubation or immobilization has not been performed, the process is resumed until a favorable response is obtained.

Next, the functionality of the sensors will be tested, and if these steps have been performed properly, the answers will be given by Nyquist Diagrams. They show the variation of the imaginary impedance (capacitive reactance) depending on the variation of the real impedance (electrical resistance). If non-conformable answers ("N") were obtained from the tests, the device is not functional.

### 8.3. Electrochemical impedance spectroscopy

The redox solution used for the three cell types was the same: **5mM Fe (CN)<sub>6</sub><sup>4-</sup>** and **5mM of Fe (CN)<sub>6</sub><sup>3-</sup>** (ferrocyanide and ferricyanide). At the same time, a saline phosphate buffer solution (PBS) was used, **pH = 7,1, frequency range: 100 kHz – 0,1 Hz.**

S-introduced G protein (BSA), left to incubate for 30 minutes and then rinsed the chips by making two washes in phosphate buffer solution. From the overlapping curves shown in Figs. 8.5, it is found that the sensor has stability, by the fact that several measured cycles overlap perfectly.

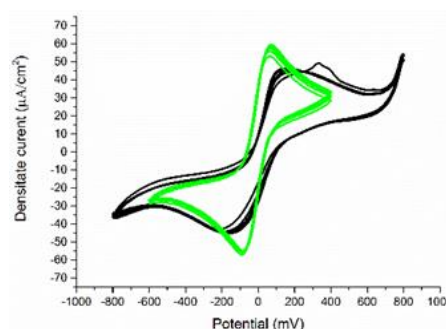


Fig. 8.5. Cyclic voltammetry curves

The next step was to **immobilize specific antibodies for each subpopulation**. 40  $\mu\text{L}$  anti-CD4 (anti-CD4, anti-CD8 and anti-CD3) concentration 5  $\mu\text{g} / \text{ml}$  was incubated and incubated for 18 h at 4  $^{\circ}\text{C}$ . In the next step, after the addition of antibody concentrations, antigens (CD3+, CD4+ and CD8+) of different known concentrations were introduced into the phosphate buffer solution (PBS = 7,1). The purpose of EIS data analysis is to determine the nature of electrode processes and their characteristic parameters. For CD4+, concentrations between 0 - 800 ng / ml shown in the Nyquist diagram were used (Fig. 8.6).

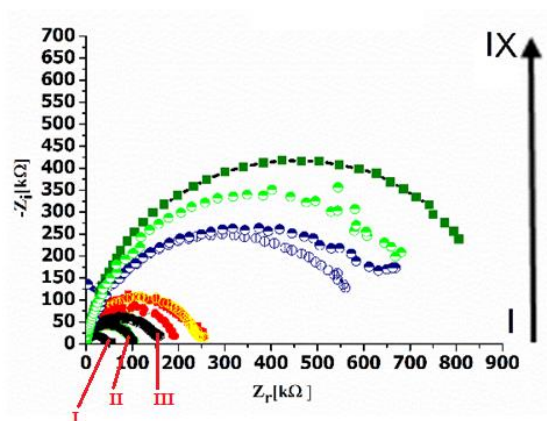


Fig. 8.6. Nyquist diagrams ( $-Z_i$  vs  $Z_r$ ) after addition of known CD4 + concentrations (introduced into phosphate buffer, pH = 7,1) [M16]

where the added antigen concentrations are:

- I. black saline phosphate buffer (0 ng / ml);
- II. black 12.5 ng / ml;
- III. black 25 ng / ml;
- IV. red 50 ng / ml;
- V. orange 100 ng / ml;
- VI. light blue 200 ng / ml;
- VII. dark blue 300 ng / ml;
- VIII. varnish 400 ng / ml;
- IX. green 800 ng / ml.

For CD3+, concentrations between 0 - 100 ng / ml shown in the Nyquist diagram were used (Fig. 8.7). It can be seen that the parabolas have increased with increasing concentrations, where the concentrations of added antigens are:

- I. red simple saline phosphate buffer (0 ng / mL);
- II. green 0.3 ng / ml;
- III. pink 0.75 ng / ml;
- IV. black 1.87 ng / ml;
- V. varnish 6.25ng / ml;
- VI. brown 25 ng / ml;
- VII. blue 50 ng / ml;
- VIII. gray 100ng / ml

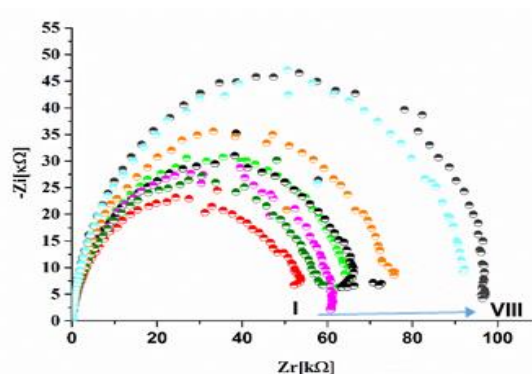


Fig. 8.7. Nyquist diagrams ( $-Z_i$  vs  $Z_r$ ) after addition of known CD3 + concentrations (introduced into phosphate buffer, pH = 7,1) [M16]

All sensors behaved similarly, the mean values for CD4 + and CD3 +  $R_{ct}$  being  $50,16 \pm 5 \text{ k}\Omega$  and the  $R_{ct}$  values recorded for CD8 + being  $10,40 \text{ k}\Omega \pm 0,10 \text{ k}\Omega$ . These mean values were determined by measuring ten electrodes and using the same procedure. The coefficient of variation between measurements was less than 15 %. From the Nyquist diagrams, the load transfer resistances (radius of each semicircle) are taken for each concentration, and from the value of the capacitive reactance, the capacitance of the electric double layer ( $C_{dl}$ ) is determined.

Electrodes functionalized for the detection of CD8+ antigens could detect differences in concentrations at the level of picograms per milliliter, as seen in Fig. 8.8.

For the CD8+ subpopulation, the sensors behaved differently from CD3+ and CD4+, in the sense that the average electron transfer resistance at the electrode-electrolyte interface was

lower. This may be due to the higher porosity of the antigen, pores that allow easier penetration of redox ions.

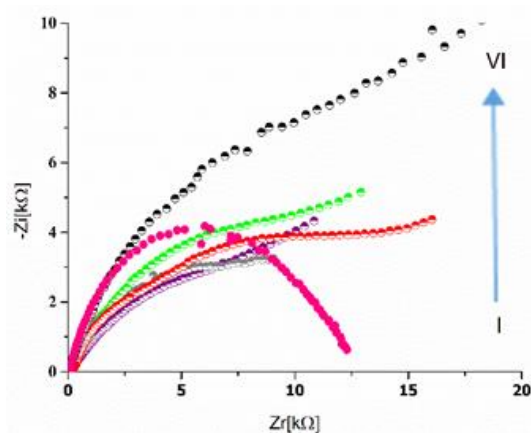


Fig. 8.8. Nyquist diagrams ( $-Z_i$  vs  $Z_r$ ) after addition of known CD8 + concentrations (introduced into phosphate buffer, pH = 7,1) [M16]

where the added antigen concentrations are:

- I. purple - 0 ng/ml;
- II. gray - 31,25 pg/ml;
- III. red- 62,5 pg/ml;
- IV. varnish - 125 pg/ml;
- V. pink - 250 pg/ml;
- VI. gray - 1000 pg/ml.

It is observed from Fig. 8.6 that at higher concentrations (1 ng / mL) other effects appear at the interface with the electrode, namely diffusions of ionic species, but the sensor responds to low concentrations of added antigens (of the order of pg / mL). Figures 8.6 - 8.8 show an increase in charge transfer resistance and a decrease in the capacity of the electric double layer with antigen concentration. The calibration curves (Fig. 8.9 - 8.11) were constructed based on the normalized electrochemical signal obtained from the Nyquist diagrams and the answers given by  $R_{ct}$  - the electronic transfer resistance at the interface given by the potentiostat software. In the calibration curves the resistance of the charge transfer for the electrolyte was noted with  $R_{ct0}$ , and with  $R_{cti}$  the resistance of the charge transfer corresponding to each concentration. Antigen concentrations were placed on the horizontal axis of the graphs, and the  $R_{cti} / R_{ct0}$  ratio on the vertical axis. The resistance of the load transfer increases in proportion to the increase in the number of cells (concentration). Depending on the size of the load transfer resistance at a certain concentration of a cell type, their number is determined.

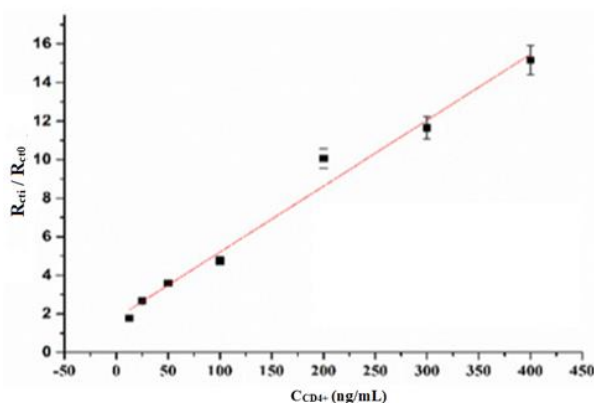


Fig. 8.9. Normalized resistive calibration curve ( $R_{cti} / R_{ct0}$ ) as a function of CD4 + concentration: Linear model with added concentrations, the concentration range being between 0 ng / mL - 400 ng / mL,  $R^2 = 0,979$  [M18], [S13]

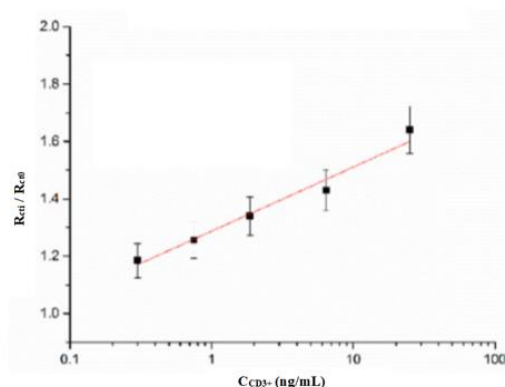


Fig. 8.10. Normalized resistive calibration curve ( $R_{cti} / R_{ct0}$ ) as a function of CD3 + concentration: Linear model with added concentrations, the concentration range being between 0 ng / mL - 25 ng / mL,  $R^2 = 0,966$

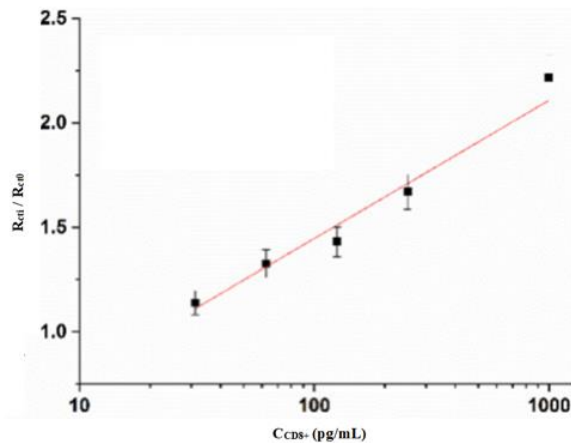


Fig. 8.11. Normalized resistive calibration curve ( $R_{cti} / R_{ct0}$ ) as a function of CD8 + concentration: Linear model with added concentrations, the concentration range being between 0 ng / mL - 1000 pg / mL,  $R^2 = 0,958$

The resistance to electronic transfer is directly proportional to the logarithm of the added concentration. The response given by the electrode with the buffer without the introduction of antigens was considered the noise ( $R_{ct0}$ ) while the response given by the standards ( $R_{cti}$ ) is the signal recorded for each concentration.

The  $R_{cti} / R_{ct0}$  ratio was calculated and represented by the logarithm of each antigen concentration. In other words, each  $R_{cti} / R_{ct0}$  ratio corresponds to a certain concentration, and each concentration corresponds to a certain number of cells, so by extrapolation, each  $R_{cti} / R_{ct0}$  ratio corresponds to a certain number of cells.

Under optimal conditions, by this method, a linear regression curve (Fig. 8.9) with a correlation coefficient ( $R^2$ ) of 0,979 was obtained when the concentration range is between 0 and 800 ng / mL for CD4 +.

A linear regression was obtained with the logarithm of each CD3+ concentration added, with a correlation coefficient of 0,966 (Fig. 8.10).

In the case of CD8 + detection, antibody concentrations were expressed in pg / mL, so the difference from one concentration to another is very small compared to the other two antigens where the concentration ranges were on the order of nanograms.

## CHAPTER 9. MANUFACTURE AND TESTING OF THE IMPROVED PROTOTYPE OF THE MICRO-ELECTRO-MECHANICAL DEVICE

### 9.1. Problems appeared in the manufacture of the micro-electro-mechanical device, experimental model

Following the stages of intermediate and final inspection of the technological process of manufacturing the micro-electro-mechanical device, experimental model, those critical (deficient) stages of the technological process were identified. Thus, it was found that:

- there was no good adhesion of the silver to the gold substrate;
- good adhesion of the SU-8 photoresist to the silicon substrate was not achieved.

In order to eliminate the critical stages found, which represent a high degree of importance, the technological process was improved in the next stage of the research-development process.

### 9.2. Improvements in the manufacturing process of the micro-electro-mechanical device

Following the tests and verifications performed, the stages of improving the manufacturing process of the micro-electro-mechanical-prototype device were established. Thus, optimizations of the technological stage of silver deposition and deposition of the photoresist SU-8 were made.

### 9.2.1. Silver deposition improvements

To eliminate the problems encountered during the execution of the device, electrochemical sensors have been replaced with sensors containing interdigitated working electrodes.

The deposition surface was modified, replacing the surface with a size of 10 nm with a larger surface of 200 nm, which allowed to fix the problem of silver adhesion. On subsequent intermediate inspections of the prototype manufacturing process, it was found that the silver did not come off the surface of the reference electrode. This type of sensor was chosen because it has the advantage of increased sensitivity.

### 9.2.2. Improvements needed to increase the adhesion of the SU-8 photoresist

Regarding the adhesion of the photoresist SU-8, the heat treatment process has been improved. Table 9.1 shows the comparison between the heat treatment steps for the SU-8 photoresistor performed previously and the improved ones.

Table 9.1. Stages of display, exposure and heat treatment to SU-8 deposition and their improvement

	Treatment performed	Improved treatment
<b>Display:</b>	4000 rot/min	3000 rot/min
<b>Heat treatment performed after the display stage:</b>	3 min - 65 °C	3 min - 65 °C
	6 min - 45 °C	6 min - 95 °C
<b>Alignment / Exposure (12 s)</b>		
<b>Heat treatment performed after the exposure stage:</b>	2 min - 65 °C	2 min - 65 °C
	7 min - 45 °C	7 min - 95 °C
<b>Development:</b>	1 min 30 s ± 10 s	3 min
<b>Final heat treatment:</b>	30 min - 180 °C	30 min - 250 °C

### 9.3. Execution of the improved prototype of the micro-electro-mechanical device

For the new device, an improved prototype, four masks were used, as follows:

- First mask (M1) - making titanium-gold sensors;
- The second mask (M2) - making silver reference electrodes;
- The third mask (M3) - deposition of a passivation oxide layer;

This newly introduced mask in relation to the previous technological process, related to the experimental model, aimed to use the oxide layer as an intermediate layer between the arms of the working electrodes made of gold and the microfluidic channel, because there was an area where they were overlaid. In order to avoid direct contact between the two areas, this layer was deposited.

- The fourth mask (M4) – the realization of the microfluidic part with the help of the photoresist SU-8.

In Fig. 9.1 the stages of the technological flow for the new device are presented, where: 1 represents the choice of the silicon substrate; 2 - silicon oxide deposition stage; 3 - deposition of the photoresist by using the first mask; 4 - depositing the Ti-Au layer; 5 - the lift-off process; 6 - deposition of the photoresist by using the second mask; 7 - deposition of the Ag layer; 8 - the lift-off process; 9 - deposition of the oxide layer by using the third mask; 10 - oxide corrosion; 11 - deposition of the photoresist SU-8 by using the fourth mask; 12 - removing the PDMS cover.

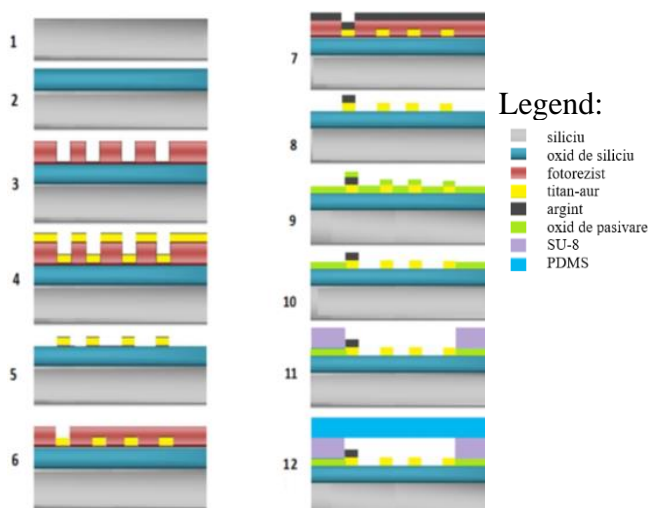


Fig. 9.1. Technological flow [M17]

### 9.3.1. Design of the micro-electro-mechanical device, improved prototype

The design of the improved prototype was done in the CleWin5 program. Compared to the experimental model, for which three masks were designed, for this new device were designed four masks.

#### First mask - the design of titanium-gold sensors

Mask 1 (M1) covers the four identical micro-electro-mechanical devices (Fig. 9.2). This mask contains the electrochemical sensors: the input measuring sensors and the output measuring sensors, the material used for these sensors being titanium-gold. In Fig. 9.3. the enlarged image of one of the four devices is shown.

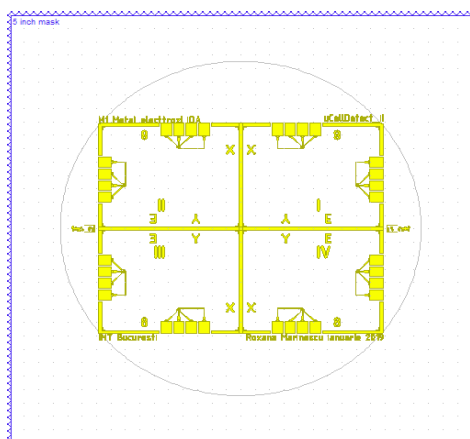


Fig. 9.2. The first designed mask (M1) of the micro-electro-mechanical device

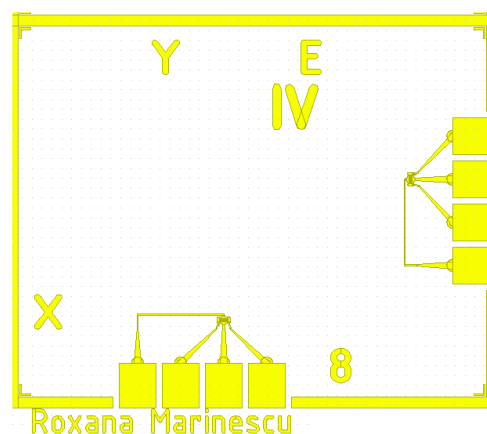


Fig. 9.3. Projected enlarged image of the area of a device on the M1 mask

The mask on which the sensors were designed contains four devices, measuring  $31400 \mu\text{m} \times 39500 \mu\text{m}$ . Each sensor has in its composition four pads (supports),  $3000 \mu\text{m} \times 3700 \mu\text{m}$ , with equal distance between them, of  $500 \mu\text{m}$ . With the help of these pads the electrical connection is made. Electrochemical sensors are made using three types of electrodes, as in the previous case, of the experimental model. These are: the working electrode (WE), the reference electrode (RE) and the counting electrode (CE).

The working electrode was made of two pairs of metal electrodes in the shape of a comb. The width of the reference electrode was  $200 \mu\text{m}$ , and that of the counting electrode was  $195 \mu\text{m}$ . The dimensions established for the working electrodes were [M17]: The size of a digit -  $20 \mu\text{m}$ ; The length of the digits -  $285 \mu\text{m}$ ; Distance between digits -  $5 \mu\text{m}$ ; The width of a digit -  $10 \mu\text{m}$ . In Fig. 9.4, the enlarged image of the electrochemical sensor can be seen.

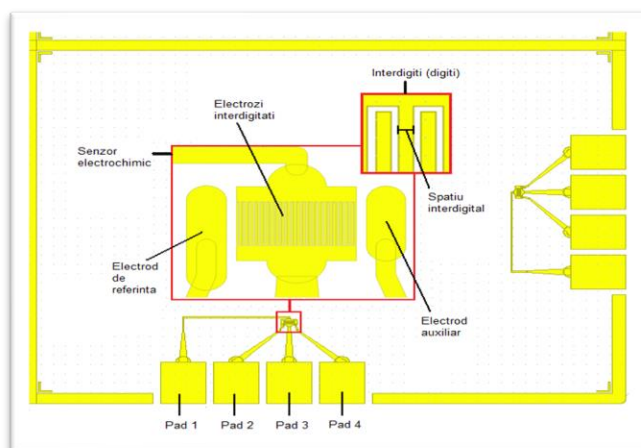


Fig. 9.4. Projected magnified image of the sensors on the first mask (M1)

### The second mask designed for making silver reference electrodes

Fig. 9.5 shows an image of the second mask, designed in CleWin5. Given the fact that on a normal scale, the reference electrode is not visible, an enlarged image of the electrode is shown in Fig. 9.6.

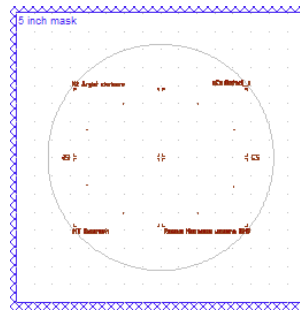


Fig. 9.5. The second designed mask (M2) of the micro-electro-mechanical device

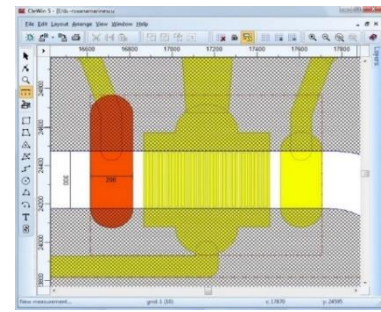


Fig. 9.6. Projected enlarged image of the reference electrode

### Third mask designed for the deposition of a layer of hydrogen silsesquioxane layer (HSQ)

This operation consisted in depositing an oxide on the entire surface of the platelet, leaving free only the contact areas and the portion where the microchannel passes over the sensor and electrodes.

Fig. 9.7 is shows an image of the third designed mask, where the arrangement of the four devices is observed. Fig. 9.8 shows the area related to a single micro-electro-mechanical device, on an enlarged scale.

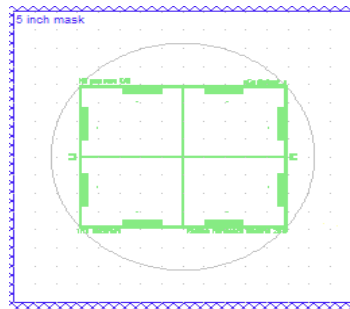


Fig. 9.7. The third designed mask (M3) of the micro-electro-mechanical device

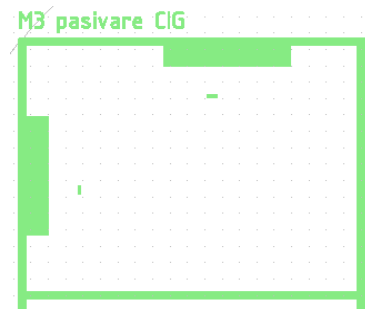


Fig. 9.8. Projected enlarged image of the area of a device on the M3 mask

### The fourth mask designed for the realization of the microfluidic part with the help of the photoresist SU – 8

The fourth mask (M4) has been designed for the realization of flow microchannels, selection and capture chamber and counting channels (Fig. 9.10).

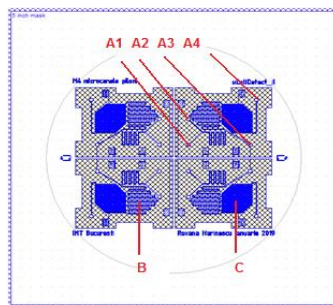


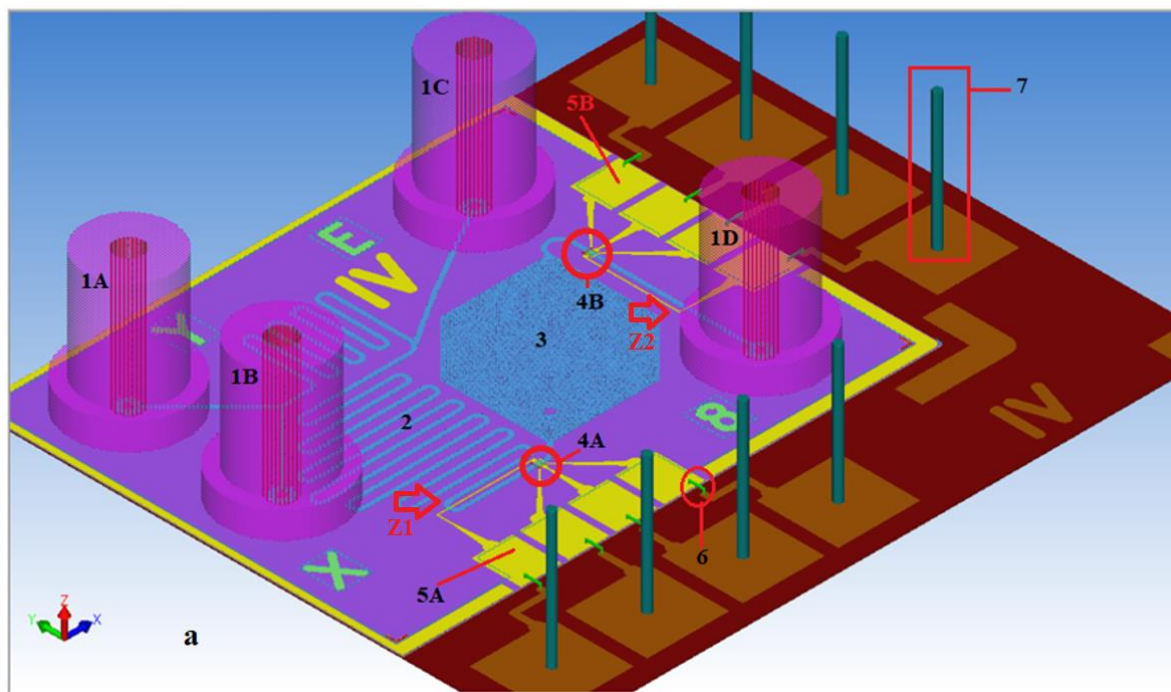
Fig. 9.10. The fourth projected mask (M4) of the micro-electro-mechanical device

The mask includes:

- A. Four nanoports:
  - A.1. For blood;
  - A.2. For erythrocyte lysis solution of blood;
  - A.3. For lysis stop solution;
  - A.4. For storing the remaining cells
- B. Microchannels;
- C. Selection and capture chamber.

### 9.3.2. Modeling of the manufacturing process of the micro-electro-mechanical device, improved prototype

The modeling of the manufacturing process of the improved prototype was done with the help of the SEMulator3D Manager program.



where:

1A represents the nanoport for blood introduction;

1B - nanoport for introducing the lysis solution;

1C - the nanoport for introducing the lysis stop solution;

1D - nanoport for collecting cell debris / solutions;

2 - microchannel;

3 - selection and capture chamber;

4A - input counting sensor;

4B - output counting sensor;

5 (A, B) - forests for electrical connection;

6 - gold threads;

7 - supports for electrical connections.

Z1, Z2 - the areas where the contact between the electrode and the microchannel would have been made, if the M3 mask had not been designed.

### 9.3.3. The manufacturing process of the masks

The masks were made with the help of DWL-66fs equipment [\*9], [\*17]. Following the stages of the previously established technological flow, after obtaining the masks, the actual manufacture of the device was approached.

Table 9.3 shows the four 5-inch photolithographic masks used to make the device.

Tabelul 9.3. The four masks of the microfluidic device, improved prototype

Design	Fabrication	Design	Fabrication
<b>Mask M1:</b> 		<b>Mask M3:</b> 	
<b>Mask M2:</b> 		<b>Mask M4:</b> 	

### 9.3.4. Execution of the micro-electro-mechanical device, improved prototype

For the manufacture of the micro-electro-mechanical device, improved prototype, a batch of four silicon wafers with orientation  $\langle 111 \rangle$  and with a size of 4 inches, diameter of 100 mm and a resistivity of  $1 \sim 10$  ohm cm, was used as substrate for manufacturing (Step 1).

This was followed by the deposition of a layer of thermally raised silicon dioxide (100 nm) in a dry medium at  $1000\text{ }^\circ\text{C}$  in the Centrotherm E1200 HT furnace (Germany) [\*17] (Step 2). The  $\text{SiO}_2$  layer serves as an insulation layer between the p-type silicon and the metal layers. The first mask was used to define the sensor electrodes on the negative photoresist ma-N 1420 (Step 3). It was deposited with the help of the Suss MicroTec spinner [\*17] (Fig. 9.20) at 3000 rpm. After deposition of the photoresist, a 2-minute heat treatment took place in the Heraeus oven [\*9], [\*31] heated to  $100\text{ }^\circ\text{C}$  (Fig. 9.21). High temperature treatments improve the adhesion of the photoresist.



Fig. 9.20. Display of the negative photoresist ma-N 1420



Fig. 9.21. Heat treatment in Heraeus oven

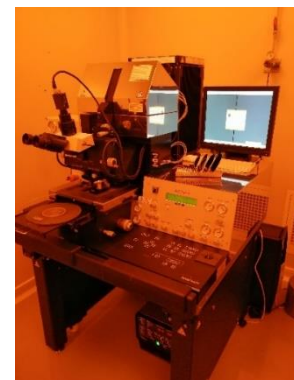


Fig. 9.22. MA6 / BA6 alignment and exposure equipment

For all photolithography processes, the same MA6 / BA6 SUSS MicroTec alignment and exposure equipment was used as in the previous [\*9], [\*17] (Fig. 9.22). The alignment was done using the signs inscribed on the masks (Fig. 9.23). The exposure lasted a few seconds

(Fig. 9.24). The last stage of the photolithography process was given by the development of the photoresist for 1 min and 5 s in the specific developer, ma-D 533 / S (Fig. 9.25).

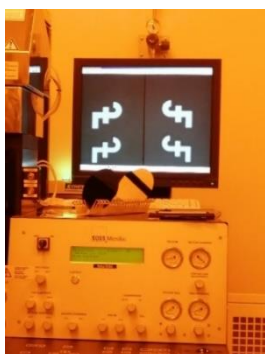


Fig. 9.23. Alignment performed using the alignment marks



Fig. 9.24. Mask exposure



Fig. 9.25. Development with ma-D solution

The photoresist that was not covered by the mask was exposed to UV and then removed, leaving the areas where the next material was deposited free. After the photolithography process, a thin layer of Ti-Au (30 nm - 300 nm) was deposited on the entire surface of the wafer. Metal deposition was done by spraying, using Neva-EVD 500A equipment (Step 4) [\*9]. The unwanted material was removed by the lift-off process (Step 5). In this case, the platelets were immersed in a container filled with acetone and a substance used for disposal (“negative remover”) (Fig. 9.26). The photoresistor used as sacrificial material was detached and removed together with the material deposited on it (Fig. 9.27). The thickness of the metal layer deposition always depends on the subsequent lift-off process [M17].



Fig. 9.26. Wafer immersion in the lift-off solution

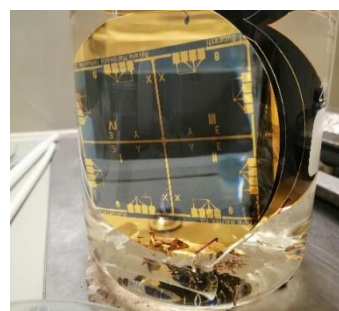


Fig. 9.27. The lift-off process

After the lift-off process, the intermediate inspection took place, performed using the Leica DM LM optical microscope (Leica Microsystems, Germany) [\*9], [\*29]. In Fig. 9.29 the sensors can be seen at different magnifications. ***All prototype devices subject to intermediate inspection have been shown to comply.***

After the Ti-Au layer was deposited, a second layer of negative photoresist was deposited (Step 6) in order to print the image on the second mask. The deposition of 100 nm of silver was performed by evaporation with the electron beam, the equipment used being Neva-EVD 500A [\*9] (Step 7). Another lift-off process followed, so that the silver remained deposited only on the reference electrode (Step 8) of the interdigitated sensors.

Ag chlorination, with the aim of stabilizing the electrodes, was done using a strong oxidant,  $\text{FeCl}_3$ . After Ag deposition, each wafer was soaked in 1 % aqueous ferric chloride for 20 minutes.

After the deposition step, the intermediate inspection was performed using the Leica DM LM optical microscope (Leica Microsystems, Germany) [\*9], [\*9]. Images of the intermediate inspection are presented in Fig. 9.33, captured at magnification of x10 and x5.

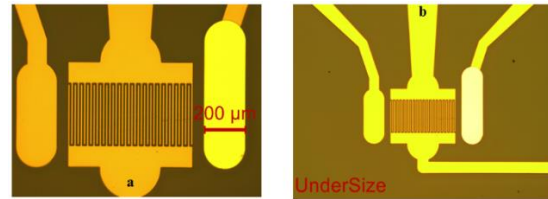


Fig. 9.33. Ag deposition a) x10 magnification image and b) x5 magnification

The third mask was used to cover the entire surface with a passivation oxide, called "hydrogen silsesquioxane" (HSQ) (Step 9), leaving the areas near the sensors and the pad area (to make future connections) free. what takes place the corrosion process (Step 10).

For this mask, 100 nm HSQ was deposited at 1000 rpm. A 2 min heat treatment was performed at 250 °C, after which a layer of HPR 504 positive photoresist was deposited at 3000 rpm. Subsequently, another heat treatment of 1 min at 100 °C was performed. Then, the third mask (4,5 s) was aligned and exposed. The photoresist was developed in the developer HPRD, while HSQ was removed using hydrofluoric acid with ammonium chloride for 15 s .

After corrosion, the intermediate inspection took place, using the Leica DM LM optical microscope (Leica Microsystems, Germany) [\*9], [\*29]. In Fig. 9.35 two x5 magnification images of the two sensors are played: the input sensor and the output sensor.

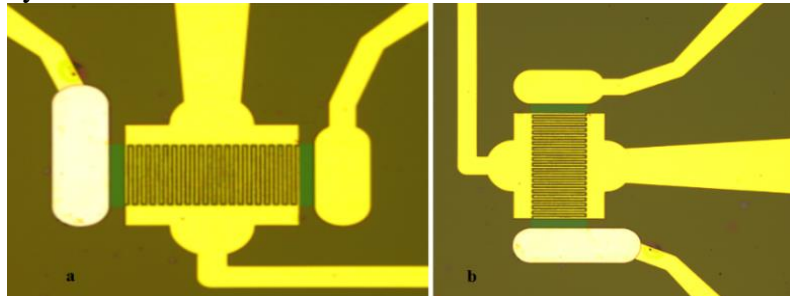


Fig. 9.35. Oxide deposition a) input sensor [M17], b) output sensor

The fourth mask was used to make the microfluidic part: the microfluidic channels and the pylons in the selection and capture chamber. For this step, a 50 nm layer of negative photoresist SU-8 2050 was deposited at 3000 rpm (Step 11). A 3 minute heat treatment was performed at 65 °C, then raising the temperature to 95 °C for another 6 minutes. Then the fourth mask was exposed (10 s), followed by another heat treatment (2 min - 65 °C and 7 min - 95 °C).

After the development in which the photoresist was removed (1 min, 30 s), the final heat treatment was performed at 250 °C for 30 min using Torrey Pines Echo Term HS60-2 [\*9], [\*35] to strengthen the photoresist SU-8. After these steps were performed, the deposits made were observed microscopically. The intermediate inspection of the microchannel, nanoports and pylons in the capture chamber took place, using the Leica DM LM optical microscope (Leica Microsystems, Germany) [\*9], [\*29] (Fig. 9.38).

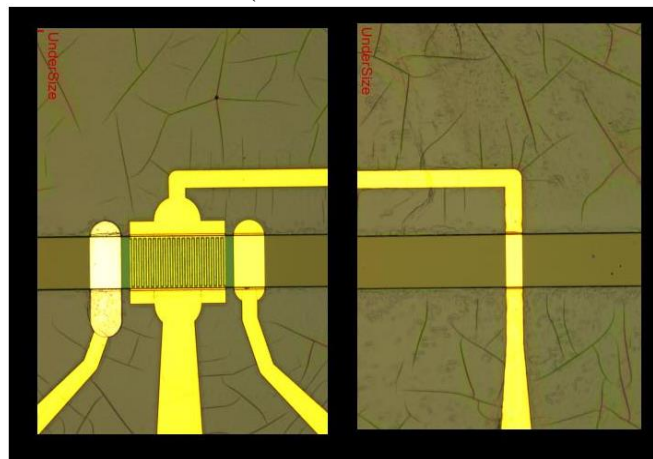


Fig. 9.38. Images of the microchannel and sensors, magnification x5

The last step (Step 12) was to make the PDMS cover, which was positioned above the device. It must not cover the electrical contacts (pads).

A thicker PDMS cover was chosen to ensure the stability of the nanoparticles. The cover is attached to each individual device after the devices have been separated by the DAD 322 cutting equipment [\*17].

One wafer was used for experimental purposes. The PDMS cover was deposited by the previously used method, for the realization of the micro-electro-mechanical device, experimental model. A thinner layer was applied in order to be able to make a comparison in terms of the resistance of the platelets to environmental effects.

After the PDMS was deposited in the specific support, it underwent a heat hardening treatment. Once reinforced, two devices were positioned over it to mark the shape to be cut. After being cut and subjected to plasma treatment, the PDMS was attached to the micro-electro-mechanical devices, improved prototype. After hardening the PDMS, the holes for the nanoparticles were drawn using a special syringe used for microfluidic holes. Then, the nanoparticles were glued with a resin. With this stage, the technological process of manufacturing the improved prototype of the microfluidic device for the determination of T lymphocytes was completed, after which the realized prototypes were subjected to specific functioning tests. In Fig. 9.47. is presented an image of the microfluidic device with the attached nanoports.

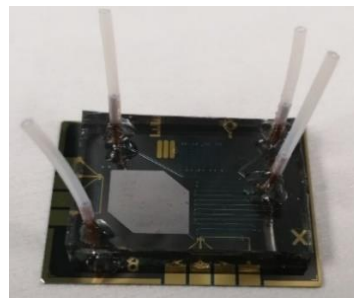


Fig. 9.47. Enhanced prototype microfluidic device with nanoparticles attached

#### 9.4. Testing the improved prototype of the micro-electro-mechanical device

The testing of the micro-electro-mechanical device, improved prototype, was performed according to the methodological steps, established in Fig. 9.48. These steps are similar to those of the experimental model, to which those related to microfluidic flow and mechano-climatic reliability tests are added.

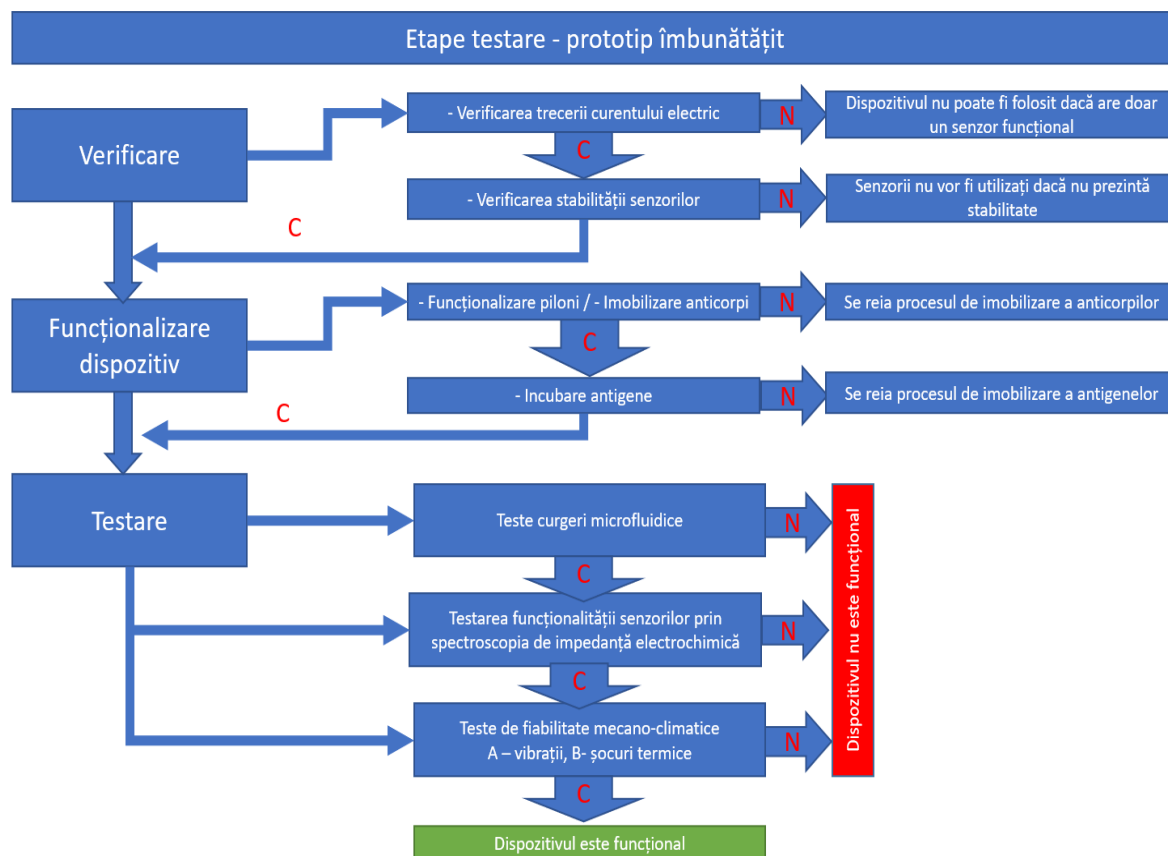


Fig. 9.48. Stages of testing the micro-electro-mechanical device, improved prototype

During the "Verification" stage, devices with functional sensors are selected that allowed the current to pass, followed by checking their stability. If the sensors are unstable, they will not be used because they will give different results for each test. For unstable sensors, the response will be marked "N" (nonconformable). These sensors will no longer be used.

When testing the improved prototype, the tests performed were performed on the same equipment as the experimental model, Keithley 2700 Multimeter / Data Acquisition System equipment (Keithley, USA). All sensors have received the compliant rating.

For functional sensors, the response was marked "C" (according to) and proceeded to the next stage, the functionalization of the device. During this step, antibodies were attached, and subsequently, different concentrations of CD3+, CD4+, CD8+ antigens were incubated. After being left to incubate, the sensors were checked. If immobilization and incubation have taken place, proceed to the next stage. Otherwise, the two immobilization / incubation operations are performed again.

The fluid flow tests precede the functionalization tests and have as object the verification of the complete passage of the microfluidic circuits with critical areas in which the sensors are positioned at the entrance and exit of the selection and capture chamber, as well as the chamber itself.

The functionality of the compliant sensors was tested using the electrochemical impedance spectroscopy method. If the answers given by the Nyquist diagrams are favorable, proceed to the mechano-climatic testing stage of the device.

If the device meets all test procedures, then it is a functional device. If unfavorable answers to one of the tests are recorded, the device is not functional.

#### 9.4.1. Sensor stability

The testing of the stability of the sensors was performed with the help of the potentiostat from the IMT equipment [\*9]. The three electrodes - the reference electrode, the counting electrode and one of the working electrodes were connected to the equipment by means of pliers (Fig. 9.49.a).

For testing, a drop of specific solution was placed over the area of interest of each sensor using a pipette (Fig. 9.49.b). The redox solution used was the same as when testing the experimental model:  $5\text{mM Fe (CN)}_6^{4-}$  și  $5\text{mM de Fe (CN)}_6^{3-}$  (ferrocyanide and ferricyanide).

In Fig. 9.50.a and Fig. 9.50.b. images of the redox solution deposited on the areas of interest of the input and output sensors are presented.

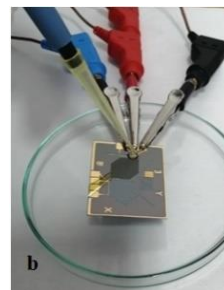
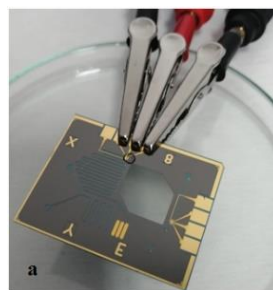
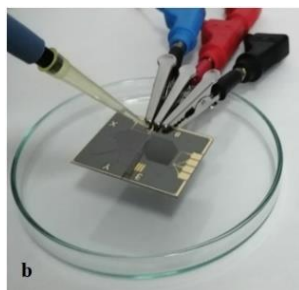
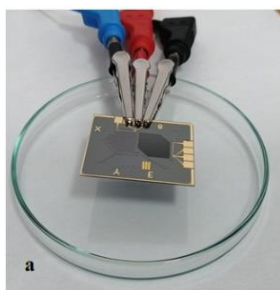


Fig. 9.49. Preparation of sensors for impedance testing a) attaching pliers to make connections, b) pouring a drop of redox solution using a pipette

Fig. 9.50. The drop of redox solution deposited on the area of interest of the measuring sensor a) inputs, b) outputs

After the redox solution drop was deposited, cyclic voltammetry diagrams were made. Figs. 9.51 and 9.52 show the cyclic voltammetry curves for the two sensors, which were obtained at the same frequency range:  $1\text{ mHz} - 0,1\text{ KHz}$ . The applied potential was:  $-0,2 \div 0,2\text{ V}$ , at a scanning speed of  $0,05\text{ V / s}$ .

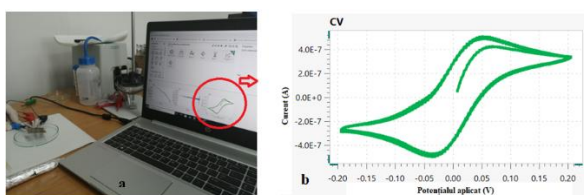


Fig. 9.51. Determination of cyclic voltammetry curves for the input sensor  
a) the PGSTAT204 potentiostat; b) cyclic voltammetry curves.

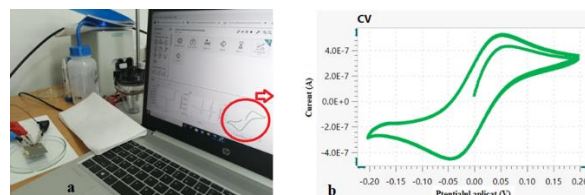


Fig. 9.52. Determination of cyclic voltammetry curves for the output sensor  
a) the PGSTAT204 potentiostat; b) cyclic voltammetry curves.

In each of the graphs shown in Figs. 9.51.b and 9.52.b., several curves are performed at a scan speed of  $0,05 \text{ V / s}$ . The perfect overlap of cyclic voltammetry curves indicates the stability of the sensors. If the sensors are not stable (do not show repeatability of measurements), they cannot be used.

#### 9.4.2. Microfluidic flow testing

Fluid flow testing is performed after functionalizing the surface of the PDMS cover and after it has been attached to the device. A dye was used to check the microchannel flow system (Fig. 9.53). The dye was introduced through each individual nanoport.

If the flow of fluids had not taken place through microchannels, it would have led to the conclusion that there is no tight closure of the lid.

In this situation, it would have been necessary to resume the treatment of plasma surface functionalization.

By this test, the modeling and simulation with finite elements of the flow in the microfluidic circuits presented above was validated.

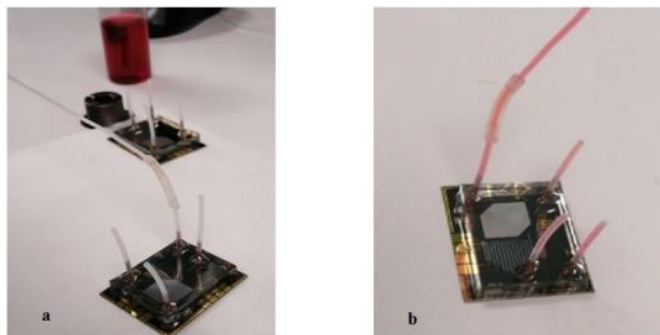


Fig. 9.53. Fluid flow test a) image before the introduction of the dye and b) image after the introduction of the dye

#### 9.4.3. Testing the sensor's functionality with electrochemical impedance spectroscopy

- **Impedance measurements**

To verify antibody immobilization and antigen quantification, impedance spectroscopy was used by recording Nyquist diagrams. The EIS measurements took place at equilibrium potential (potential generated between electrodes immersed in the electrolyte), at a frequency range between  $100 \text{ mHz} - 100 \text{ kHz}$ .

Figures 9.54 - 9.56 show the Nyquist graphs after G protein immobilization, antibody immobilization and after reaction with specific antigen concentration. In these experiments, the electrodes were functionalized with the G protein, which is porous, which is why the charge transfer resistance occurs only at high frequencies (tens of kHz), and at lower frequencies ion diffusion phenomena occur. These effects are reflected in the Nyquist diagrams in Figures 9.54 - 9.56 in which very small radius semicircles appear in the area of high frequencies followed by curves with large radii of curvature at lower frequencies. In Fig. 9.54 are presented the graphs

for the CD3+ subpopulation, and in Fig. 9.55 are presented the graphs for the CD4+ subpopulation.

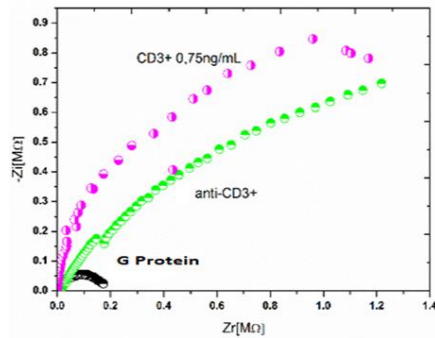


Fig. 9.54. Nyquist diagrams for CD3+ antigen [M17]

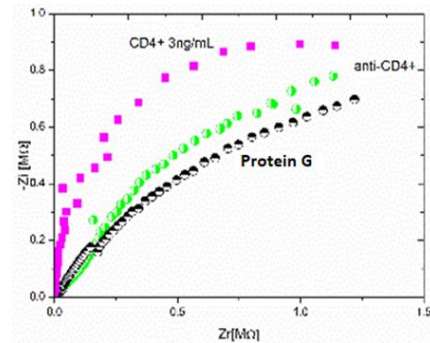


Fig. 9.55. Nyquist diagrams for CD4+ antigen [M17]

In Fig. 9.56 graphs for the CD8+ subpopulation are presented.

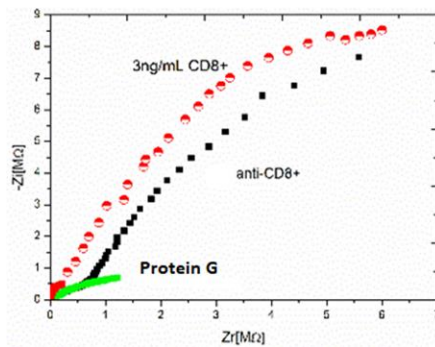


Fig. 9.56. Nyquist diagrams for CD8+ antigen [M17]

The load transfer resistance for protein G was noted with  $R_{ct0}$ , and with  $R_{ct}$  the load transfer resistance corresponding to each antigen (CD3+, CD4+, CD8+). Where:  
For CD3,  $R_{ct} / R_{ct0} = 0,85 / 0,07 = 12,14$ ;  
For CD4,  $R_{ct} / R_{ct0} = 0,9 / 0,7 = 1,28$ ;  
For CD8,  $R_{ct} / R_{ct0} = 8,5 / 0,6 = 14,16$ .

From the electrochemical impedance spectra, it was found that the micro-electro-mechanical device, an improved prototype, has a high sensitivity for detecting the number of T lymphocytes.

In case of functionalization, in order to detect the subpopulations CD3+, CD4+, CD8+, it was possible to detect a difference between resistances even when the differences between concentrations were very small, of the order of ng / ml.

### 9.5. Integration of the microfluidic chip into a portable device

The small mass and dimensions (Fig. 9.57 - 9.59) make the micro-electro-mechanical device, an improved prototype, manufactured to allow its integration into a portable device.



Fig. 9.57. Determination of the mass of the micro-electro-mechanical device, improved prototype

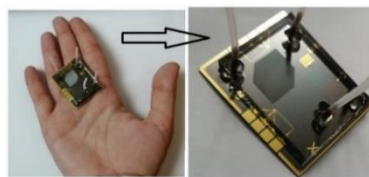


Fig. 9.58. Improved prototype of the physically made micro-electro-mechanical device

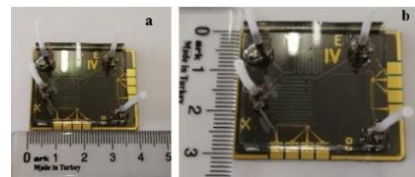


Fig. 9.59. Dimensions of the microfluidic device a) length, b) width

The fact that this device used for cell detection is portable is a major advantage. In order for the testing with the help of the micro-electro-mechanical device not to take place only in the specialized centers / institutions that have special equipment for determining the impedance, a solution of this problem was sought.

The device can be connected to a data acquisition board, equipped with a microcontroller specialized in impedance spectroscopy. This board can convert and analyze the data obtained using impedance. The micro-electro-mechanical device was connected to the board by binding with gold wires. In turn, the card is connected to a computer via a USB cable. Then install the software and run the program. The same frequency range used for the equipment with which the device was tested is used, which is set from the computer (Fig. 9.60).

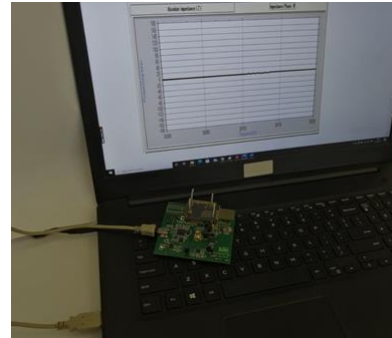


Fig. 9.60. Connecting the control board to the laptop via USB cable

The interpretation of the results is done using the calibration curves obtained by specialized medical institutions, testing several patients - a mandatory requirement for a statistical interpretation [O3].

## 9.6. Mechanical-climatic reliability tests for the micro-electro-mechanical device

Reliability tests are of major importance in the development of a portable MEMS device [B7].

One of the attributes required for portable devices is the increased reliability. In order to demonstrate the ability and efficacy of the microfluidic device to be used as a portable device, tests were performed under similar or similar stress conditions to those encountered in a real operating environment [T1].

### A. Vibration tests

A vibration test is very important in the case of a portable device, which can be transported by various means, whose drive motors can induce vibrations. The micro-electro-mechanical device by its nature has a certain degree of fragility, which can generate false results. The equipment used for vibration testing was “Shaker Tira TV 55240 / LS-180” and “Amplifier Tira A101 1 010” (Tira, Germany) [\*17].

After the microfluidic device was placed in the support made by additive manufacturing (Fig. 9.63), the support was fixed in the Tira equipment. Attaching the support with screws to the vibration test equipment is shown in Fig. 9.64.

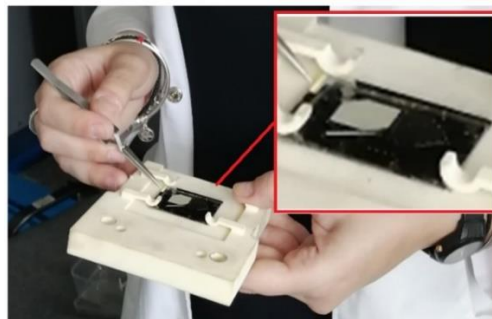


Fig. 9.63. Attaching the device to the holder made using 3D printing technology



Fig. 9.64. Vibration testing of micro-electro-mechanical device

The tests were performed based on the standards 6AA-TE 100535 and PM-LEM-10 Ed 8 Rev 3 [\*19], at an ambient temperature of 25 °C and a relative humidity of 37 %. The parameters set for vibrations were:

- from 20Hz to 80 Hz +3dB/octava, 0,04 G<sup>2</sup>/Hz;
- from 80Hz to 350 Hz; 0,04 G<sup>2</sup>/Hz;
- from 350Hz to 2kHz -3dB/octava.

The graphs resulting from the tests are presented in Fig. 9.65 and in Fig. 9.66.

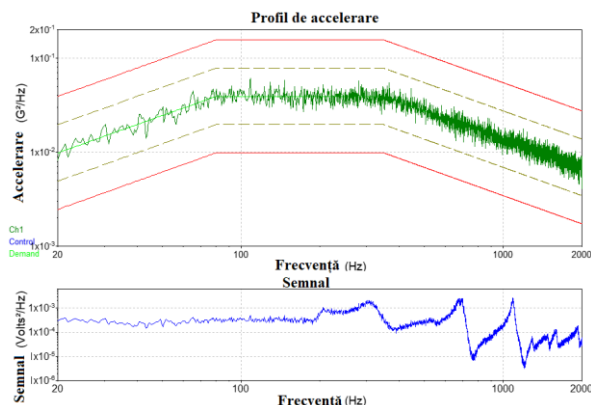


Fig. 9.65. Random vibration results on the X axis

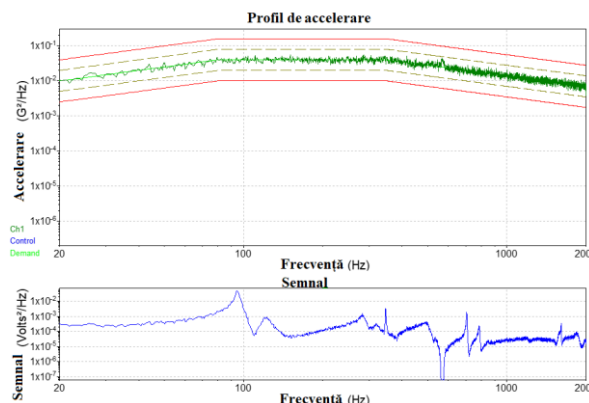


Fig. 9.66. Random vibration results on the Y axis

The values obtained for the test that lasted 1:10:38, operating at a maximum level of 100 % for 10 minutes are presented in Table 9,5, as well as the channel frequencies.

Following the results obtained, it was established by visual and microscopic examination that the device had not been damaged.

Table 9.5. Parameters obtained in vibration tests

Frequency	G <sup>2</sup> /Hz	dB/Octave
20 Hz	0.009829	3
80 Hz	0.03913	0
350 Hz	0.03913	-3
2000 Hz	0.006889	
<b>Axa x</b>		
Ch2	0.002628 G RMS	0.001016 G RMS
Ch3	0.004935 G RMS	0.001976 G RMS
Ch2	20 mV/G	
Ch3	11 mV/G	
<b>Axa y</b>		
Ch2	0.003346 G RMS	0.000997 G RMS
Ch3	0.005038 G RMS	0.001913 G RMS
Ch2	20 mV/G	
Ch3	11 mV/G	

## B. Thermal shock tests

Temperature and humidity tests are considered key factors of tests similar to those in the real environment [B7]. These thermal shock tests, according to MIL-STD-810 standards, were performed to see if the PDMS cover came off the micro-electro-mechanical devices, improved prototype [\*19]. For these tests, two devices were used, with PDMS cover of different thicknesses, one with a layer of approx. 5 mm and another with a thin layer with a thickness of approximately 1 mm (Fig. 9.67). Temperature tests consisted of performing six thermal cycles from -30 °C to +60 °C,

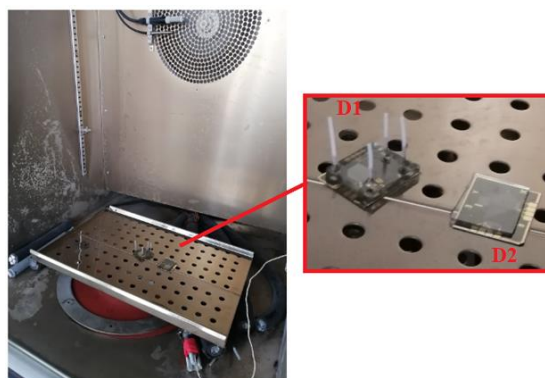


Fig. 9.67. Introduction of the two samples in the test chamber, where D1 - mechanical micro-electro device with thick layer of PDMS, and D2 - micro-electro mechanical device with thin layer of PDMS.

using CH 250 Angelantoni equipment (Agilent Technologies, USA) [\*17].

This equipment contains a climate chamber in which the temperature and humidity are controlled. In this type of room, combined tests can be performed: vibrations + climatic conditions. The temperature range is between -40 °C and +180 °C. The relative humidity range is 20 - 95% (between 10 and 80 °C), and the maximum heating / cooling rate is 2 °C / min. The tests on the CH 250 Angelantoni equipment (Fig. 9.68.a.) are performed using specific standards (Fig. 9.68.b).

In Table 9.6, the data obtained from the thermal cycles are presented.

After the end of the six thermal cycles, the two micro-electro-mechanical devices (D1, D2) were removed from the test chamber and their inspection was performed.

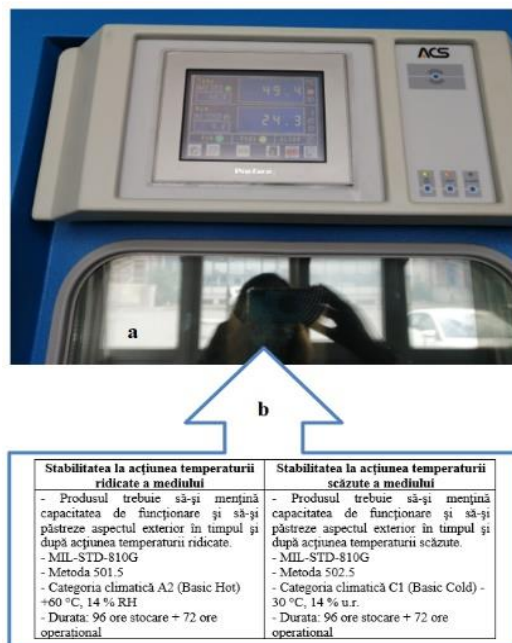


Fig. 9.68. Thermal testing a) CH 250 Angelantoni equipment interface, b) MIL-STD-810G requirements

In Table 9.6, the data obtained from the thermal cycles are presented.

Table 9.6. Parameters of thermal cycles performed

Time [min]	05	10	15	20	25	30	35	40	45	50	55	60
Temperature [°C]	-25,2	-27,1	-8	16	37,3	55,5	27,2	3,6	-8,5	-14,8	-19,4	-22,8
Humidity [%]	31,4	33,7	95	67	33,3	21	10,7	14,4	18,3	21,2	24,7	28,4

It was found that the device D1 - with thick PDMS cover did not undergo any modification, while D2 - with a thin layer of PDMS, had places where the PDMS layer came off, as can be seen in Fig. 9.70.

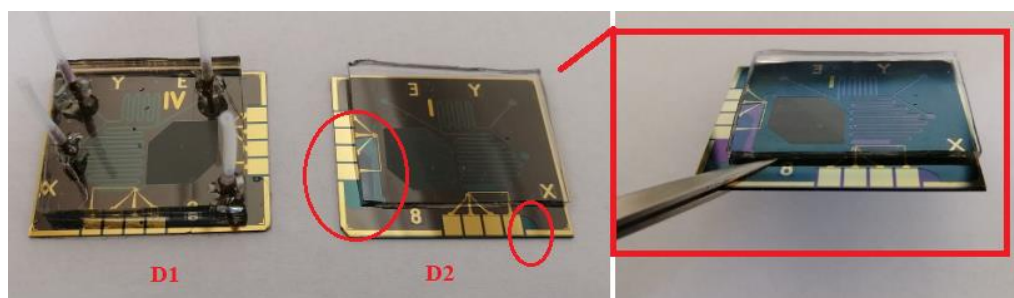


Fig. 9.70. Inspection of the two devices after the thermal cycles

Thus, following the intermediate inspection, it was decided to use the PDMS cover with a layer of 5 mm thickness, which withstood large temperature variations, far exceeding the usual conditions of use, laboratory.

The realized micro-electro-mechanical device passed from the development stage (TRL2) to the manufacturing stage, which was validated in the laboratory (TRL4). Reliability tests performed in conditions similar to or close to those in the actual operating environment have created conditions for transition to higher maturity levels, TRL 5 and TRL 6 [\*32], [\*36].

## 9.7. Development of a humidity sensor for monitoring the storage conditions of the micro-electro-mechanical device

Due to the fact that the problems encountered in the manufacture of the micro-electro-mechanical device may be due to humidity, it was decided to make a humidity sensor with a new sensitive layer. The sensor is intended to be much improved over existing sensors on the market. It can be used as an independent device to monitor humidity in the rooms where the technological processes take place. The new sensitive layer was made of polyvinylpyrrolidone (PVP) and oxidized carbon nanohorns - oxCNH (1/1, w / w) [Ş1]. The sensor was tested for humidity, using as a comparison a commercial humidity sensor - Sensirion. Good RH sensitivity of sensors compared to commercial sensor, when RH varies from 0% to 90% in humid air environment [M15].

The thickness of the deposited layer was measured with Nova NanoSEM 630 equipment (FE-SEM, FEI Company, USA) [\* 17]. This was about 200 nm. The nanohorns are placed next to each other, occupying the free spaces as the number of layers increases, thus forming a continuous layer (Fig. 9.81 - 9.83) [M25].

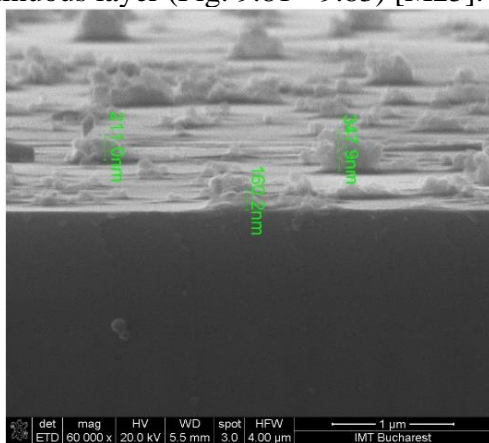


Fig. 9.81. SEM images for the single layer sample [M25]

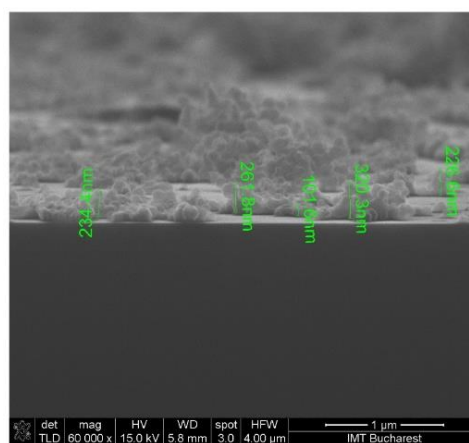


Fig. 9.83. SEM images for the eight-layer sample [M25]

The use of the new sensitive layer film gives the sensor several significant advantages, among which: superior mechanical properties; rapid response to variations in relative humidity; increased sensitivity; stability; small size; reasonable production costs. To demonstrate its reliability in extreme operating conditions, relevant mechano-climatic tests have been performed. The device has been tested for vibration and thermal shock from - 30 °C to + 60 °C. No tests were identified following the tests performed.

Thus, a new functional humidity determination sensor has been developed, with a sensitive layer composed of oxidized carbon nanowires and PVP, which can be used to monitor the manufacturing stages of micro-electro-mechanical devices or can be integrated in the protection / storage housing. of micro-electro-mechanical devices.

## CAPITOLUL 10. FINAL CONCLUSIONS, PERSONAL CONTRIBUTIONS AND FUTURE RESEARCH DIRECTIONS

### 10.1. Final conclusions

Following the critical analysis of the current state of the field approached in the first part of the thesis and the development of research activities in the second part on the realization of the experimental model and the improved prototype of the microfluidic device for determining T lymphocytes, the following final conclusions were drawn:

1. BioMEMS are applicable to the determination of T lymphocytes having several main advantages over conventional equipment, which consist in: reducing the volume of samples; energy consumption and low costs; portability and reuse of devices; fast sample processing and implicitly short reaction time for diagnosis and treatment.

2. Materials used in the construction of bioMEMS are classified into substrate and deposition materials. Silicon is widely used in the form of substrate and metals, metal compounds, ceramic and polymeric materials, as deposition materials. The new trend of development of bioMEMS is related to carbonic materials, represented by graphene and its derivatives, nanocorns and carbon nanotubes, etc.

3. The microtechnologies used in the manufacture of bioMEMS, in various stages, some even in the case of the realization of the microfluidic device for the determination of T leukocytes are:

- the photochemical processing achieves high precision, based on the photolithography process for the selection of the surfaces to be processed with the help of masks, using photoresist substances; has the advantage of high productivity due to the simultaneous sampling of the material on the entire surface exposed to the process of selective chemical corrosion;

- laser radiation processing (LBM) is used for the direct writing of masks, by using lasers with short wavelength, in the UV field, ensuring a small diameter of the spot and implicitly a high energy density on the processed surface;

- electron beam processing (EBM) is used for lithography by direct writing (matrix scanning of the surface) and beam design by electromagnetic deflection, but also for the deposition of materials in the composition of bioMEMS in thin layers;

- ion beam processing (IBM) is used to deposit materials from the structure of bioMEMS in thin layers or to remove material in the form of dry corrosion, by “Reactive Ion Etching” (RIE) and “Deep Reactive Ion Etching” (DRIE);

- Plasma Enhanced Chemical Vapor Deposition (PECVD) is used for the deposition of materials in the form of thin films, for example, amorphous SiC (A-Si) and vertical graphene (VG), used as cell culture substrates in applications bioMEMS.

4. The bio-device for counting type T lymphocytes from designed and modeled blood is structured in the following component parts: (1) nanoparticles for introducing the blood sample, erythrocyte lysis solution, lysis stop solution; (2) microfluidic circuits for erythrocyte lysis and for lysis arrest; (3) CD3 +, CD4 + or CD 8+ leukocyte selection and capture chamber; (4) electrochemical impedance sensors for counting cell inputs and outputs into and out of the selection and capture chamber; (5) cell storage tank at the exit of the selection and capture chamber.

5. For the experimental model of the microfluidic device, three masks were designed in the CleWin5 program: (1) for titanium-gold deposition; (2) for depositing silver; (3) for deposition of the photoresistor SU-8; the manufacturing process of the experimental model was modeled using the SEMulator3D program.

6. The numerical modeling and simulation of the flow of the three types of fluids in the lysis and stop lysis circuits, in the counting channels corresponding to the electrochemical sensors and in the selection and capture chamber was performed in Comsol Multiphysics; the simulation results showed that the designed geometry meets the time conditions for traversing the microfluidic circuits to achieve the erythrocyte lysis process and stop lysis; the results obtained were validated following subsequent functional tests, post-manufacture.

7. The *experimental model* of the microfluidic device was manufactured using a batch of five silicon wafers, on which four devices (20 pieces) were arranged, based on the sequence of steps previously modeled using SEMulator3D. After each stage of manufacture, intermediate inspections were carried out, removing non-compliant products. At the end of the

manufacturing process, only nine microfluidic devices remained - experimental model compliant.

8. The *experimental model* of the microfluidic device was tested based on the developed test methodology, going through several stages; checking the electrical conductivity of the sensors; checking the operational stability of the sensors and finally, their functionality. The functionality of lab-on-a-chip devices for the electrochemical detection of the three lymphocyte subpopulations was demonstrated: CD4 +, CD3 + and CD8 +, which is the main objective of the doctoral thesis: the manufacture of a functional bioMEMS device to determine the number of T lymphocytes in blood.

9. Following the inspection of the quality of the execution stages of the micro-electro-mechanical device, *experimental model*, two major problems were identified which led to critical non-conformities: (1) lack of adhesion of silver to the silicon wafer; (2) lack of adhesion of the photoresist SU-8 to the plate.

10. These problems were solved when making the *improved prototype* of the microfluidic device for the determination of lymphocytes by: increasing the surface size of the reference (interdigitated) electrodes on which the silver was deposited; improving the heat treatment of the wafer on which the photoresist SU-8 was deposited.

11. To increase the sensitivity of the T-cell detection process, a new prototype device was generated in the CleWin5 program, an *improved prototype* phase, obtained by integrating interdigitated electrochemical sensors on the microfluidic platform. The manufacturing process was modeled again in the SEMulator3D program, the results obtained being validated at the post-manufacturing tests of the prototype.

12. For the *improved prototype* of the microfluidic device, four masks were manufactured: (1) for depositing the titanium-gold layer used in the construction of the sensors; (2) for depositing the silver layer for the reference electrode; (3) for the deposition of an oxide layer that has blocked the contact between the gold and the microchannel in unwanted areas; (4) for the deposition of the photoresist SU-8 with the help of which the microfluidic circuits were made.

13. Applying the developed methodology for testing the *improved prototype*, steps similar to those related to the experimental model were followed, to which were added the testing of microfluidic flow and testing the functionality of sensors by electrochemical impedance spectroscopy. Following the analysis of the obtained Nyquist diagrams, it was found that the micro-electro-mechanical device can detect with *high sensitivity* the three lymphocyte subpopulations: CD4 +, CD3 + and CD8 +, which is the confirmation of obtaining the main objective of the doctoral thesis.

14. The microfluidic device for the determination of T lymphocytes was integrated in a portable device and subjected to specific reliability tests, vibrations and thermal shocks. The results obtained, close to those encountered in a real operating environment, presented the required compliance of such equipment.

15. Research steps were taken that made the transition from the technological maturity level, TRL2, the concept phase of the microfluidic device for determining T lymphocytes to the technological maturity level, TRL 4, the validation phase of the operation and manufacturing technology of the microfluidic device at laboratory level and premises were created for the transition to the levels of technological maturity TRL 5 and TRL 6, by validating the operation of the device in similar conditions, respectively close to those encountered in the real operating environment.

## 10.2. Original contributions

Analyzing the results of research conducted in the doctoral thesis entitled "Manufacturing processes of micro-electro-mechanical systems with applications in medicine"

highlights the following original contributions, developed on the two main categories, *theoretical* and *applied*, as follows:

**A. From a theoretical point of view:**

- characterization of the major trend in the technological field of miniaturization and ultraminiaturization, namely, micro and nanotechnologies and selection of the most appropriate such technologies applicable in the manufacturing process of micro-electro-mechanical bio-devices;
- classification and characterization of MEMS, with a focus on those used in the medical field - bioMEMS;
- classification and characterization of the components of Micro-Electro-Mechanical Systems and selection of those components suitable for the construction of *lab-on-a-chip* devices, respectively biosensors, microfluidic circuits, nanoports and micropumps for the introduction of analyzed samples and reactants;
- in the characterization of micro-electro-mechanical systems are highlighted the connections with the human factor, which is the object of analysis, using attachable or implementable devices, such as nanorobots or unmanageable devices or using bioMEMS and interpreting the results obtained;
- identification of post-manufacturing tests, necessary for the current use of micro-electro-mechanical bio-devices, in conditions as close as possible to those encountered in reality and fulfilling the reliability requirements;
- analysis of the properties of materials usable for MEMS in terms of critical conditions necessary for the construction and manufacture of bioMEMS: adequate mechanical and electrical characteristics, adaptability to semiconductor manufacturing technology and properties that limit the development of internal stresses during micro-processing, necessary to generate surfaces for microfluidic circuits;
- characterization of the materials applicable for bioMEMS, as well as their grouping according to their properties, in *substrate* and *deposition* materials; identifying their advantages and disadvantages in relation to the specificity of bioMEMS and the compatibility between them;
- in order to increase the performance of bio-devices, the current trend of use for new generation technologies of carbon materials with exceptional thermal, optical, mechanical and electrical properties, associated with extremely low mass - materials represented by graphene and its derivatives, nanowires and carbon nanotubes, etc .;
- selection of those unconventional advanced technologies, also called concentrated energy technologies, which by their ability to create high energy densities on the processed surface are the most suitable for Industry 4.0; in this context, they are also applicable to the manufacture of ultra-miniaturized bioMEMS;
- were classified, phenomenologically characterized and highlighted those technologies with concentrated energies, the most appropriate materials for each technological stage and their critical parameters for obtaining MEMS according to requirements, as well as the types of equipment used, highlighting their advantages and disadvantages in the processes of manufacturing - technological flow;
- a new trend in microtechnology was identified, applicable to bioMEMS, in various stages of the technological manufacturing process, through the wider use of laser radiation processing in conditions of continuous decrease in equipment costs, the ability of technology to create the greatest energy density in the industrial field and processing of extremely different types of materials and microgeometers;
- characterization of microfluidics and highlighting its ability to use micro-electro-mechanical devices applied in the medical field; selection and characterization of the most suitable

materials to be used for microfluidic devices, as well as highlighting the diversity of the morphology of microfluidic circuits;

- the current state of lab-on-a-chip devices was characterized, the relevant solutions reported following the research-development-innovation activities worldwide were highlighted and in this context, the location of the microfluidic device for determining T lymphocytes, made in the thesis for the first time in Romania, in the hierarchy of similar devices;
- a research methodology was developed for a micro-electro-mechanical device for the determination of T lymphocytes, which led to the transition from the level of technological maturity, TRL2, the concept phase to the level of technological maturity, TRL 4, the validation phase the operation of the device and the manufacturing technology at laboratory level, with the creation of the premises for the transition to the levels of technological maturity TRL 5 and TRL 6, by validating the operation in similar conditions, respectively close to those encountered in the real operating environment;
- a methodology for testing a microfluidic device was developed, framed in the holistic process of its manufacture - design, modeling, simulation, execution, testing, delivery. The methodology includes the general steps related to sensor testing by verifying electrical conductivity, stability in operation, fluid flow testing in microfluidic circuits, functionality testing by capturing cells undergoing lab-on-a-chip analysis and reliability mechano-climatic testing.

## B. From a practical point of view

Following the experimental research carried out, the following contributions were made to the doctoral topic, grouped in two major stages of development of the microfluidic device for the determination of T lymphocytes, experimental model and improved prototype, as follows:

### Experimental model

- The conceptual design of the micro-electro-mechanical bio-device was performed, applicable to determine the number of T-type lymphocytes in the blood samples, formulating the general function, main and secondary functions, elaborating its logic diagram with the main components: sample inputs blood and lysis and stop lysis solutions, microcircuits of erythrocyte lysis process and stop lysis process modules, counting channels associated with electrochemical sensors, positioned ante and post capture chamber, T lymphocyte selection and capture chamber, reservoir of accumulation of residual cells from the blood sample;
- Design of an experimental model of the micro-electro-mechanical bio-device for determining the number of T-type lymphocytes in the blood samples; this involved computer modeling to determine the critical shape and dimensions of some essential elements of the microfluidic part such as: lysis circuits and lysis stop solution, counting channels, capture chamber with pillar sizing and distance between them;
- Design and computer modeling of the three masks required in the photolithography stage within the technological process of manufacturing the experimental model, namely: mask 1 used to deposit the Ti-Au layer; mask 2 for Ag deposition; mask 3 used to make the microfluidic part using SU-8, a negative photoresist;
- Numerical flow modeling, following the variation of the flow rate and fluid pressure in the specific lysis and anti-use modules of microfluidic circuits, in the counting channels and inside the T lymphocyte selection and capture chamber, which demonstrated the operation of the micro-electro biodevice -mechanic in the design phase and subsequent validation of the computerized results with the real data obtained from the tests performed;

- Computerized modeling of the manufacturing process of the experimental model of the MEMS bio-device and validation of the results obtained from the actual manufacturing process and testing of the physical model, by verifying the prescribed functional parameters;
- A batch of 20 pieces was executed in the *experimental model* phase of the MEMS bio-device, identifying those non-compliant devices based on intermediate inspections, as well as the critical technological stages of the manufacturing process in order to improve in the subsequent *prototype* phase;
- A test methodology for the microfluidic device was developed and applied, an *experimental model*, which included the following successive steps: testing of sensors on electric current flow and stability in operation, testing by electrochemical impedance spectroscopy after functionalization on antibody attachment and incubation of different concentrations of antigens.

### Improved prototype

- Improving the MEMS bio-device for the determination of T lymphocytes through the following functional and technological measures:
  - changing the previous sensors with those composed of interdigitated electrodes;
  - increase of the Ag deposition surface, corresponding to the sensors made of this material;
  - the introduction of the third mask, in the intermediate technological stage corresponding to the deposition of a passivation oxide layer, which aims to block the contact between the arms of the new sensors and microchannels in unwanted areas, in order to avoid false answers given by sensors;
  - modification of the parameters of display, development and heat treatment to increase the adhesion of the negative photoresist, SU-8;
- Computerized modeling of the new technological manufacturing process of the improved prototype of the MEMS bio-device with the subsequent validation of the results obtained through the experimental data from the final testing;
- Development and application of an *improved prototype* testing methodology, which also includes testing of fluid flow in microfluidic circuits, sensor functionality, as well as mechano-climatic reliability tests;
- Integration of bioMEMS for the determination of T lymphocytes in a portable device and testing of the final product, in laboratory conditions, at mechanical and thermal stresses, in conditions close to actual use;
- A humidity sensor with increased sensitivity in relation to similar products on the market was designed, modeled, made and tested, used to monitor the storage conditions and use of the micro-electro-mechanical device for the determination of T lymphocytes;
- A micro-electro-mechanical device was made for the determination of T lymphocytes, passing through the stages of technological development, the concept stage - Technology Readiness Level- TRL 2, to the manufacturing technology phase, validated in the laboratory- TRL 4;
- Through the reliability tests to which the micro-electro-mechanical device for determining T lymphocytes was subjected, in similar operating conditions, respectively close to those encountered in reality, the premises for transition to TRL 5 maturity levels were created and TRL 6;
- An important leap has been made, towards the essential stage of making a product, ready to be launched on the market, from *pre-competitive* research to *competitive* research. The latter creates the conditions for achieving the competitive advantage of an innovative organization;

- A micro-electro-mechanical device was manufactured with a series of advantages such as: ultra-miniaturization, very low energy consumption, complex functionality, portable and reusable and implicitly, low manufacturing and operating costs;
- The original contributions resulting from the design, modeling, manufacturing simulation and experimentation activities indicate that the device called “Portable microfluidic biochip for determining the number of T lymphocytes” with the presented characteristics and advantages, obtained in the doctoral thesis, was made for the first time. in our country.

It is mentioned that these application contributions would not have been possible without using the available technical-material base, the equipment provided by the National Institute for Research - Development for Microtechnology - IMT Bucharest (IMT) and the expertise gained in this advanced field, within IMT.

### 10.3. Future directions of research

Microtechnology is a leading field, in a continuous evolution, generating new products, which improve our quality of life. Due to the evolution of 'micro' and 'nano' technologies, there has been a substantial increase in the complexity of equipment and devices used in various fields, especially in medicine, at all stages specific to the medical act.

Particular attention needs to be paid to bioMEMS, these devices with integrated biological functions, used for medical applications. At present, there is an amazing demand for autonomous microdevices in the medical field, with the implicit need for miniaturized energy sources. For example, as a result of the impact of the COVID 19 pandemic, bioMEMS had an increase in market share of about 90% in 2019-2020 [\*39].

*In this context, micro-electro-mechanical systems with applications in medicine represent a major research direction that will be further accelerated. Due to the fact that the use of the newly developed device, Portable Microfluidic Biochip to determine the number of T lymphocytes produces significant effects and results, the following directions of future research may be extended, in connection with the topic addressed in the thesis:*

- Development of new medical devices for other uses, such as the determination of circulating tumor cells (CTC), with directions to:
- The use in their composition of carbonaceous materials, used in the manufacture of MEMS, such as graphene and its derivatives;
- Studying how to obtain graphene and its derivatives, which involves:
  - a. Performing various experiments to choose the appropriate method;
  - b. Testing it embedded in devices;
- Design and modeling of other forms of microfluidic circuits, numerical simulation on their hydraulic behavior, aiming to minimize pressure losses;
- The use of other micro and nanotechnologies with concentrated energies for the manufacture of bioMEMS, leading to increased productivity, accuracy and quality of the surfaces generated, as well as further reduction of their dimensions, according to the trend of ultraminiaturization, which minimizes the volume of samples, energy consumption and cost reduction and, implicitly, increasing the market share of such high technical products.

### 10.4. Valorification of the research results

Following the bibliographic research carried out, respectively following the developments and contributions within the doctoral thesis, the author has carried out in the research field, numerous theoretical and applied studies that have materialized in scientific papers and patent applications, participation in conferences, international trade fairs, as set out in Annexes 5 to 12.

## SELECTIVE BIBLIOGRAPHY

- [A11] Avram, A.M., Avram, M., Iliescu, C., Volmer, M., *BioMEMS for the Determination of Rheological Properties of Biological Fluids*, Proceedings of SPIE, **vol. 6415**, 2007.
- [A12] Avram, A., Mărculescu, C., Bălan, C.M., Pirvulescu, C., Volmer, M., Popescu, A., Mihăilescu, M., Avram, M., *Microbionensors for electrical impedance spectroscopic study of melanoma cells*, Proceedings of International Semiconductor Conference (CAS), pp. 165-168, 2012.
- [A14] Avram, M., Avram, A., Iliescu, C., *Biodynamical analysis microfluidic system*, Microelectronic Engineering, **vol. 83**, no. 4-9, pp. 1688–1691, 2006.
- [B4] Baughman, R.H., Zakhidov, A.A., de Heer, W.A., *Carbon nanotubes--the route toward applications*, Science **vol. 297**, no. 5582, pp. 787-792, 2002.
- [B7] Băzu, M., Băjenescu, T., *Failure analysis: a practical guide for manufacturers of electronic components and systems*, Ed. Wiley, 2011.
- [B14] Bowers, N., *Mems technology for your senses*, Yole Developpement, Electronic specifier, publicat la data de 22 Sept 2015: <https://www.electronicspecifier.com/news/analysis/mems-technology-for-your-senses>, accesat la data de: 25.09.2017.
- [B15] Buiu, O., Șerban, B.C., Ionescu, O., *Internet of things and the human body*, Journal of Nanomedicine Research, **vol. 5**, no. 2, 00113, 2017.
- [C17] Comsol, *Introduction to COMSOL Multiphysics, version 5.5*, disponibil la: <https://cdn.comsol.com/doc/5.5/IntroductionToCOMSOLMultiphysics.pdf>, accesat la: 10.06.2020.
- [D1] Dascălu, D., *Școala românească de micro- și nanoelectronică*, Editura Academia Romana Bucuresti, 2018.
- [G5] Ghiculescu, D., **Marinescu, R.**, Avram, M., *Finite Element Modeling of Lab-on-Chip for T Lymphocyte Analysis*, Macromolecular Symposia, **vol. 395**, no. 1, 2021.
- [J3] Jammes, F. C., Maerkl, S. J., *How single-cell immunology is benefiting from microfluidic technologies. Microsystems & Nanoengineering*, **vol. 6**, no. 1, doi:10.1038/s41378-020-0140-8, 2020.
- [K5] Kukhta, A.V., Maksimenko, S.A., Taoubi, M.I., Harb, M., Cataldo, A., Bellucci, S., Nuzhdin, V.I., Valeev, V.F., Stepanov, A.L., *Effect of silver doping by ion implantation on graphene nanoplatelets properties*, Optoelectron. Adv. Mat., **vol. 13**, no. 5-6, pp. 354-358, 2019.
- [M2] Mack, C.A., *Positive Photoresists– Exposure*, The Lithography Tutor (Lithography Expert), Tutor 5, 1994, pp. 21-23.
- [M3] Mack, C., *Fundamental Principles of Optical Lithography: The Science of Microfabrication*, Ed. Wiley, 2007.
- [M4] Madou, M.J., *Fundamentals of microfabrication and nanotechnology – solid-state physics, fluidics, and analytical techniques in micro- and nanotechnology*, third edition, **vol. 1**, CRC Press, 2011.
- [M5] Madou, M.J., *Fundamentals of microfabrication and nanotechnology – manufacturing techniques for microfabrication and nanotechnology*, third edition, **vol. 2**, CRC Press, 2011.
- [M15] Marinescu, N.I., Ghiculescu, L.D., Popa, L., Pîrnău, C., **Marinescu, M.R.**, Ene, G.M., *Procese tehnologice cu fascicule, oscilații și jeturi*, **vol. 3**, Tehnologii cu oscilații ultrasonice, Ed. Printech București, 2019.
- [M16] **Marinescu, M.R.**, Avram, M., Voitincu, C., Savin, M., Mihăilescu, C., Ghiculescu, D., *Development of a new Biomedical MEMS for T Lymphocytes Determination*, Vision 2025: Education excellence and management of innovations through sustainable economic competitive advantage, Proceedings of 34<sup>th</sup> International-Business-Information-Management-Association (IBIMA), pp. 3209-3220, 2019.
- [M17] **Marinescu, M.R.**, Avram, M., Voitincu, C., Savin, M., Mihăilescu, C., Ghiculescu, L.D., *Electrochemical sensors with interdigitated electrodes for counting T-cells*, Romanian Journal of Information Science and Technology, **vol. 23**, no. 4, pp. 368-378, 2020.
- [M18] **Marinescu, M. R.**, David, E., *Obtaining carbon structures from organic compounds derived of biomass for their use in chemical sensors manufacturing*, Journal of Optoelectronics and Advanced Materials, **vol. 22**, no. 3-4, pp. 194-199, 2020.
- [M19] **Marinescu, M. R.**, David, E., Ghiculescu, L.D., *Obtaining of high density carbon materials by coke sintering resulting from heat treatment of tar for applications in sensors manufacture*, proceedings of ICAMS 2020 – 8<sup>th</sup> International Conference on Advanced Materials and Systems, 2020.

- [M20] **Marinescu, M.R.**, Ghiculescu, D., *Technological aspects regarding the use of photolithography in obtaining micro-electro-mechanical systems (MEMS)*, Nonconventional Technologies Review, **vol. 21**, no. 1, pp. 24-29, 2017.
- [M21] **Marinescu, M.R.**, Ghiculescu D., *Micro-electro-mechanical systems (MEMS) and applications in medicine*, Nonconventional Technologies Review, **vol. 21**, no. 4, pp. 10-17, 2017.
- [M22] **Marinescu M. R.**, Ghiculescu, L.D., *Detection of modified cells using "lab-on-a-chip (LOC)" microfluidic devices*, Nonconventional Technologies Review, vol. **22**, no. 2, pp. 25-30, 2018.
- [M23] **Marinescu, M.R.**, Avram, M., Pîrvulescu, C., Voițincu, C., Țucureanu, V., Matei, A. *Considerations regarding the use of SU-8 photoresist in MEMS technique*, Nonconventional Technologies Review, vol. **22**, no. 3, pp. 10-14, 2018.
- [M24] **Marinescu, M.R.**, Șerban B., Dumbrăvescu, N., Avramescu, V., Cobianu, C., Buiu, O., *Carbon-based materials for healthcare micro-devices*, Nonconventional Technologies Review, **vol. 23**, no. 4, pp. 72-77, 2019.
- [M25] **Marinescu, M.R.**, Șerban, B.C., Cobianu, C., Dumbrăvescu, N., Ionescu, O., Buiu, O., Ghiculescu, L.D., *"Mechanical properties of carbon-based nanocomposites for sensors used in biomedical applications"* – UPB Sci. Bull., Series B, **vol. 83**, Iss. 1, pp. 31-42, 2021.
- [M27] Marshall D., *The Coulter Principle: Foundation of an Industry*, JALA: Journal of the Association for Laboratory Automation, **vol. 8**, no. 6, pp. 72-81, 2003.
- [M30] Mărculescu, C., Bala, C.M., Avram, A., Avram, M., *Analyzing microfluidic devices using numerical modeling*, U.P.B. Sci. Bull., Series D, **vol. 76**, no. 2, 2014.
- [M32] McLaughlin, E., Breaux, L., *Chemical Mineralogy - Smelting and Metallization*, Ed. Nova Science Publishers, Inc., 2009.
- [M33] McMillan, B., *Marele atlas ilustrat al corpului uman*, Ed. Litera, 2017.
- [M37] Moldovan, C., *Microsenzori integrați pe siliciu și tehnologii de microprelucrare*, Ed. Electronica 2000, 2004.
- [O3] Olson, S., *The role of human factors in home health care*, The National Academies Press, 2010.
- [P7] Pinto, V.C., Sousa, P.J., Cardoso, V.F., Minas, G., *Optimized SU-8 processing for Low-Cost Microstructures Fabrication without Cleanroom Facilities*, Micromachines, **vol. 5**, no. 3, pp. 738-755, 2014.
- [P10] Prime Faraday Partnership, *An Introduction to MEMS*, Ed. Prime Faraday Partnership, 2003.
- [R2] Rebello, K.J., *Applications of MEMS in surgery*, Proceedings of the IEEE, **vol. 92**, no. 1, pp. 43-55, 2004.
- [R4] Ruiz, G.P., Kristin, De Meyer, Witvrouw, A., *Poly-SiGe for MEMS - above - CMOS sensors*, Ed. Springer, pp. 1-23. 2014.
- [S5] Shah, K.A., Tali, B.A., *Synthesis of carbon nanotubes by catalytic chemical vapour deposition: A review on carbon sources, catalysts and substrates*, Materials Science in Semiconductor Processing, **vol. 41**, pp. 67-82, 2016.
- [S12] Stamatina, I., *Nanomateriale aplicații în biosenzori, surse de energie, medicină, biologie – Elemente de nanotehnologie*, Editura Universității din București, 2008.
- [S13] Stan Dana, Mihăilescu Carmen Marinela, Rădulescu Clara Hortensia, *Procedeu de funcționalizare electrochimică a unor electrozi interdigitate pentru detectia antigenului receptor de suprafața CD4+ al subpopulațiilor de limfocite T-CD4+*, DDS Diagnostic SRL, Nr. Cerere brevet A 2018 00572.
- [S14] Stanimirovic, Z., Stanimirovic, I., *Mechanical properties of MEMS materials*, Micro Electronic and Mechanical Systems (Rijeka: Intech), capitolul 11, pp. 165-176, 2009.
- [Ș1] Șerban, B.C., Buiu, O., Avramescu, V., Ionescu, O.N., Cobianu, C., **Marinescu, R.**, Pachiu, C., *Senzor chemirezistiv de umiditate pe bază de nanohornuri carbonice oxidate*, IMT București, CBI: A/00443/22.07.2019.
- [Ș2]. Șerban, B. C., Buiu, O., Cobianu, C., Avramescu, V., Dumbrăvescu, N., Brezeanu, M., Bumbac, M., Nicolescu, C.M., **Marinescu, R.**, *Ternary Carbon-Based Nanocomposite as Sensing Layer for Resistive Humidity Sensor*, in Multidisciplinary Digital Publishing Institute Proceedings, **vol. 29**, no. 1, pp. 114, 2019.
- [T1] Tănăsescu, F.T., Stefanescu, Ghe., Ilie, C., Popa, M., Dumitru, S., *Încercări de performanță pentru caracterizarea unui dispozitiv MEMS*, Buletinul AGIR, **vol. 4**, pp. 97-102, 2015.

- [Z2] Zhang, J.X.J., Hoshino, K., in *Molecular Sensors and Nanodevices: Fundamentals of nano/microfabrication and scale effect*. *Molecular Sensors and Nanodevices*, pp. 43–111, Academic Press, 2019.
- [Z4] Zhang, X., Mariano, C.F., Ando, Y., Shen, K., *Bioengineering tools for probing intracellular events in T lymphocytes*, Wiley Interdisciplinary Reviews: Systems Biology and Medicine (WIREs), pp. e1510 (1-28), 2020.
- [Z7] Zhou, W., Bridges, D., Li, R., Bai, S., Ma, Y., Hou, T., Hu, A., *Recent progress of laser micro- and nano manufacturing*, Science Letter Journal, vol. 5, no. 228, 2016.
- [\*9] \*\*\* Institutul National de Cercetare – Dezvoltare in Microtehnologie – IMT Bucuresti: [www.imt.ro](http://www.imt.ro), Echipamente ale Institutului, disponibile la: [https://www.imt.ro/echipamente/characterization\\_tools.htm](https://www.imt.ro/echipamente/characterization_tools.htm), accesat la data de 09.08.2017.
- [\*16] \*\*\*IMT București, proiect *Cellimmunochip*, disponibil la: [https://www.imt.ro/cellimmunochip/rezultate\\_etapaIII.html](https://www.imt.ro/cellimmunochip/rezultate_etapaIII.html), accesat la data de 03.02.2021.
- [\*17] \*\*\*TGE-PLAT/IMT Bucureti, *Ofertă de expertiză, servicii și echipamente pentru domeniile: microsenzori, componente fotonice, dispozitive și sisteme pentru unde milimetrice*, Ed. INCD pentru Microtehnologie – IMT București, publicat la data de Iunie 2018, disponibil la: [https://www.imt.ro/TGE-PLAT/doc/Brosura\\_TGE-PLAT\\_iunie2018.pdf](https://www.imt.ro/TGE-PLAT/doc/Brosura_TGE-PLAT_iunie2018.pdf), accesat la data de 09.12.2020
- [\*18] \*\*\*Azo materials, *Glass substrates and wafers for MEMS applications*, publicat la data de 05.10.2010, disponibil la: <https://www.azom.com/article.aspx?ArticleID=5433>, accesat la data de 03.04.2018.
- [\*19] \*\*\*FED-STD-209E, *Federal standard: airborne particulate cleanliness classes in cleanrooms and clean zones* (11 Sep. 1992) / [S/S BY ISO14644-1 and ISO14644-2], disponibil la: [http://everyspec.com/FED-STD/FED-STD-209E\\_21739/](http://everyspec.com/FED-STD/FED-STD-209E_21739/), accesat la data de 10.05.2021
- [\*20] \*\*\*Sângele - compoziție, rol, analize medicale de laborator, disponibil la: <https://bioclinica.ro/pentru-pacienti/hematologie-1/sangele-compozitie-rol-analize-medicale-de-laborator>.
- [\*23] \*\*\*Semiconductor Wafer Inc (SWI) Taiwan, produse disponibile la: <http://www.semiwafer.com/>, accesat la data de 20.05.2020.
- [\*27] \*\*\*Suss MicroTec, echipamente disponibile la: <https://www.suss.com/en>, accesat la data de 23.03.2019.
- [\*28] \*\*\*J.P. Selecta S.A., echipamente disponibile la: <https://grupo-selecta.com/fr/>, accesat la data de 23.03.2019.
- [\*29] \*\*\*Leica Microsystems, echipamente disponibile la: <https://www.leica-microsystems.com/products/>, accesat la data de 23.03.2019.
- [\*31] \*\*\*Heraeus, echipamente disponibile la: <https://www.heraeus.com/en/group/home/home.html>, accesat la data de 23.03.2019.
- [\*32] \*\*\*Technology readiness levels (TRL), disponibil la: [https://ec.europa.eu/research/participants/data/ref/h2020/wp/2014\\_2015/annexes/h2020-wp1415-annex-g-trl\\_en.pdf](https://ec.europa.eu/research/participants/data/ref/h2020/wp/2014_2015/annexes/h2020-wp1415-annex-g-trl_en.pdf), accesat la data de 05.05.2021.
- [\*33] \*\*\*IMT București, proiect Cancellab, disponibil la: <https://www.imt.ro/cancellab/rezultate.php#2016>, accesat la data de 11.12.2017.
- [\*34] \*\*\*Ocean Insight, echipamente disponibile la: <https://www.oceaninsight.com/support/software-downloads/>, accesat la data de 04.05.2021.
- [\*35] \*\*\*Torrey Pines Scientific, echipamente disponibile la: <https://www.torreypinescientific.com/>, accesat la data de 03.02.2021.
- [\*36] \*\*\* Definiții TRL, disponibil la: [https://uefiscdi.gov.ro/userfiles/file/PNCDI%20III/P2\\_Cresterea%20competitivitatii%20economiei%20romanesti/TRL.pdf](https://uefiscdi.gov.ro/userfiles/file/PNCDI%20III/P2_Cresterea%20competitivitatii%20economiei%20romanesti/TRL.pdf), accesat la: 28.06.2021
- [\*37] \*\*\* U.S. Department of Energy, *Technology Readiness Assessment Guide*, Disponibil la: <https://www.directives.doe.gov/directives-documents/400-series/0413.3-EGuide-04a>, accesat la data de: 28.06.2021.
- [\*38] \*\*\*ThermoFisher - eBioscience™ 1X RBC Lysis Buffer, Disponibil la: <https://www.thermofisher.com/ro/en/home.html>, accesat la data de: 20.01.2019.
- [\*39] \*\*\*Yole Developpement, *COVID-19: Yole's analysts point out the impacts on the bioMEMS industry*, Disponibil la: [http://www.yole.fr/BIOMEMS\\_MarketUpdate.aspx](http://www.yole.fr/BIOMEMS_MarketUpdate.aspx), accesat la data de: 25.06.2021.

**APPENDIX 1. LIST OF ABBREVIATIONS**• **General**

ADN - Deoxyribonucleic acid  
ADP - Adenosine diphosphate  
ATP - Adenosine triphosphate  
anti-CD3+, CD4+, CD8+ - specific CD3+, CD4+, CD8+ antibodies  
anti-EpCAM - anti-EpCAM antibodies  
bioMEMS - MEMS with integrated biological functions  
CE - "Counting Electrode"  
CI - "Integrated Circuits" -  
*CIRP - International Committee for Research in Production*  
Citometrie POC - "Point Of Care" citometry  
CNHs - "Carbon Nanohorns"  
CNTs - "Carbon Nanotubes"  
CTC - "Circulating Tumor Cells"  
DI - "Deionized Water"  
DRIE - "Deep Reactive Ion Etching"  
EBM - "Electron Beam Machining"  
EIS - "Electrochemical Impedance Spectroscopy"  
EpCAM - "Epithelial Cell Adhesion Molecule"  
FEM - "Finite Element Method"  
GaP - "Gallium Phosphide"  
GaAs - "Gallium Arsenide"  
GaSb - "Gallium Antenomid"  
GID - "Gold Interdigitated Electrodes"  
GOD - glucose oxidase  
GO - "Graphene Oxide"  
GQDs - "Graphene Quantum Dots"  
HIV - human immunodeficiency virus  
HPR 504 - positive photoresist called HPR 504  
HPRD - development solution  
HSQ - hydrogen silsesquioxan  
IDA/IDE - interdigitated electrodes  
IBM - "Ion Beam Machining"  
IDT - interdigitated structures  
*IMT - National Institute for Research and Development in Microtechnologies*  
LOC - Lab-On-a-Chip devices  
LBM - "Laser Beam Machining"  
LCVD - "Laser Chemical Vapor Deposition"  
LED - "Light-Emitting Diode"  
MEMS - Micro-Electro-Mechanical Systems  
NEMS - Nano-Electro-Mechanical Systems  
NK - Natural Killer lymphocytes  
ODEP - optically induced dielectrophoresis  
oxCNH – oxidised Carbon Nanohorns  
PBS - "Phosphate Buffered Saline"  
PDMS – Polydimethylsiloxane  
PDGF - "Platelet Derived Growth Factor"  
PG - Protein biomolecules  
PM - Plasma Machining  
PMMA - "Polymethyl methacrylate"  
PVDF - "Polyvinylidene fluoride"  
rGO - reduced Graphene Oxide  
RBC - "Red Blood Cells"

RE - "Reference Electrode" -  
RIE - "Reactive Ion Etching"  
SU-8 - negative photoresist called SU-8  
USM - "Ultra Sound Machining"  
UV - Ultraviolet light  
WBC - "White Blood Cells"  
WE - "Working Electrode"

- **Parameters**

A – atomic mass  
 $A_s$  – the superior deviation  
 $A_i$  – the lower deviation  
 $C_{dl}$  – the capacity of the electric double layer  
d – distance between tasks  
E – electric field intensity  
f - frequency  
G - gravity  
I - current intensity  
K - Clausius- Mossotti factor  
RMS - „Root Mean Square”  
 $R_{ct}$  – electronic transfer resistance at the interface  
 $R_{ct0}$  – load transfer resistance for the electrolyte  
 $R_{cti}$  – load transfer resistance corresponding to each concentration  
S – the surface of the interface  
t - time  
 $t_a$  – chemical attack time  
U – acceleration voltage

- **Solutions**

CD - *Differentiation cluster (refers to a cellular phenotype)*  
CD 3+ - differentiation group 3  
CD 4+ - differentiation group 4  
CD 8+ - differentiation group 8  
anti -CD3 - antibodies of the CD3 differentiation cluster  
anti -CD4 - antibodies of the CD4 differentiation cluster  
anti -CD8 - antibodies of the CD8 differentiation cluster  
BSA - bovine serum albumin  
HPRD 402 - developer for positive photoresist  
LOR 10B - photoresist called LOR 10B  
PG - G protein  
PVP - polyvinylpyrrolidone  
SAMs – mixed solutions